An Investigation of the Alloy System of Aluminium, Copper, and Zinc.

By

Hideo Nishimura.

(Received June 1st, 1927.)

CONTENTS.

PART. I.
THE CONSTITUTION OF ALLOYS OF ALUMINIUM, COPPER, AND ZINC.

INTRODUCTION.

The present work has been taken up to investigate the constitution of aluminium, copper, and zinc alloys on the side of aluminium and zinc. One part of this research was already published in Japan in the summer of the year 1925. In the autumn, however, the writer received a paper on the same problem by D. Hanson and Marie L. V. Gayler in England. (J. Inst. Metals, (1925) advanced copy). On reading it, he found in their diagram some points different from his own. So he continued his investigation, and still found that he had to give a somewhat different explanation to the diagram according to his later experiments.

The writer is now glad to have the opportunity of publishing the results of his study. Especially does he want to say that he has endeavoured to solve this ternary system from the theoretical standpoint, as he has often published his researches on such problems in Japan. He hopes that the results of the present investigation will make some contribution to the study of ternary alloys in general.

HISTORICAL REVIEW AND SOME REMARKS.

As the ternary alloy system is composed of 3 binary series, it is necessary in the first place to investigate them. But all of these binary systems composing the *Al-Cu-Zn* alloys have been already studied in detail by many investigators as described later, and we did not find any necessity to go over them again. In some cases, however, we made a few experiments on some important alloys to verify the diagram already published.

a) Aluminium-Zinc System.

Concerning this binary system, Rosenhain and Archbutt[1] published in the first place an investigation of the diagram of this system in a fairly complete form. Afterwards Bauer and Vogel[2] corrected it, and recently D. Hanson and Marie L. V. Gayler[3], W. Sander and K. L. Meissner[4], T. Hemmi[5], T. Tanabe[6], T. Ishiwara[7], and the present writer[8] published the results of their respective researches. The results of these latest experiments are almost in accordance with one another, so that we found hardly any room for further investigation.

b) Copper-Zinc System.

Cu-Zn system has been already investigated by many authors. Above all in our country, H. Imai[9] published in the year 1923 the results of his experiments in the measurement of electric conductivity. Then T. Iitsuka[10] made thermal and microscopical studies fairly in detail. The zinc side of this system, however, is not so important in industry, hence it has not received any particularly detailed study. Especially concerning the

(1) J. Inst. Metals, 2 (1911), 236.
(2) Mit. d. Kgl. Mat. pruf. Amsts, (1915), 146.
(3) J. Inst. Metals, (1922). 267.
(4) Zeit. Metallkunde, 14 (1922), 267.
(5) Industrial Chemistry, Japan, 25 (1922), 511.
(6) J. Iron and Steel, Japan, 9 (1923), 623.
(7) Investigation of Metals, Japan, 1 (1924), 283.
(8) Memoir of the College of Engineering, Kyoto Imp. Univ., 3 (1924), 133.
(9) Science Reports of the Tohoku Imp. Univ., 11 (1922), 313.
(10) Memoirs of the College of Science, Kyoto Imp., Univ., 8 (1925), 179.

solubility of zinc-rich solid solution we found only the investigation made by W. M. Pierce[1]. As the present purpose was the study of aluminium-rich alloys, we did not consider it very necessary to spend time in studying this system especially.

c.) Aluminium-Copper System.

The binary diagram of aluminium and copper was investigated by many authors, such as Gwyer, Carpenter and Edwards, Curry, Guillet, Campbell and Matthews, Merica, Waltenberg and Freeman, E. H. Dix, and so forth. In Japan, also, B. Otani and T. Hemmi[2], M. Goto and T. Mishima[3], M. Tasaki[4] made their investigations either on the whole series or on the side of aluminium.

By the researches of these authors on the aluminium rich alloys, an eutectic point between *Al* and $CuAl_2$ was found to exist at 546° C., its composition being 32 per cent. of copper, and the solubility of $CuAl_2$ in aluminium was also determined as shown in Table 1.

Table 1.

Solubility of $CuAl_2$ in Aluminium.

Temperature °C.	Solubility Cu %	Experimentists
525	4.0	Merica, etc.[5]
300	1.0	,,
540	5.0	Alloy Research Committee.[6]
300	3.5	,,
525	4.8	B. Otani.[2]
420	1.5	,,
548	5.5	E. H. Dix.[7]
430	2.0	,,

(1) Trans. Am. Inst. Min. and Met. Eng. (1922), advanced paper.
(2) J. Industrial Chemistry, Japan, 24 (1921), 1353.
(3) J. Min. Inst. Japan, 39 (1923), 714.
(4) Investigation of Metals, 2 (1925), 490.
(5) Bulletin Am. Inst. Min. Eng., (1919), 1031.
(6) Eleventh Report to the Alloy Research Committee, (1921)
(7) Trans. Am. Inst. Min. and Met. Eng., (1926), advanced copy.

Thus this system has been thoroughly investigated, but we made a few experiments for the sake of necessity, and the results of the thermal analyses are shown in Table 2, and plotted in Fig. 1.

Table 2.

Thermal Analyses of Copper and Aluminium Alloys.

No.	Composition (analysed)		Point of Change or Arrest		
	Cu %	Al %	°C.		
1	4.16	remainder	651	(583)	545
2	11.53	,,	636	(580)	547
3	19.45	,,	608		547
4	29.21	,,	564		546
5	37.50	,,	570		547
6	44.26	,,	584		547
7	50.05	,,	596		547
8	54.03	,,	610		590
9	60.19	,,	649	624	590

Fig. 1.

Cu-Al Alloys.

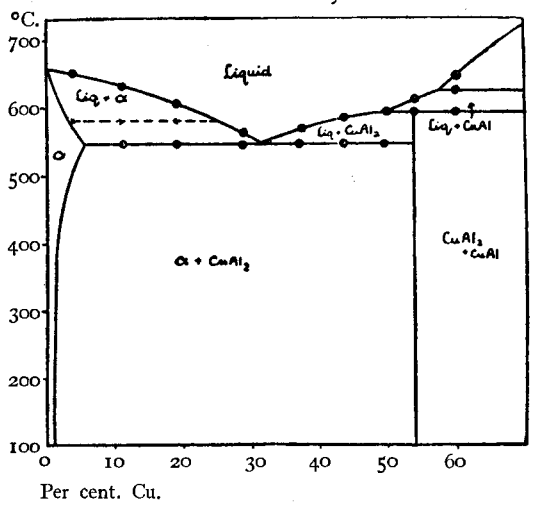

From these results it may be noted that aluminium-rich alloys containing copper less than the eutectic composition showed a slight evolution of heat at about 580° C. This evolution of heat has been already

found by B. Otani[1] and C. Sugiura[2]. C. Sugiura said it might be due to impurities contained in the aluminium, but we found also such evolution of heat more distinctly in the aluminium alloys containing copper and zinc. Therefore it seems to us that it had better be attributed to such a property of an aluminium-rich solid solution containing copper as the β transformation of iron.

Furthermore we see from the diagram that the compound $CuAl_2$ is formed under the peritectic reaction liquid + $CuAl \rightleftarrows CuAl_2$ and has no definite melting point. It agrees well with the diagram given by Jareš, Tasaki, etc.

d) The Aluminium, Copper, and Zinc System on the Aluminium and Zinc Side.

Since the research of this system was carried out by Levo Malvano,[3] we came upon no complete investigation till recently except that of V. Jareš[4], who determined the constitution of these alloys fairly extensively, although some fragmental researches had been made by Haughton and Bingham[5], and the Alloy Research Committee[6]. Finding that their results were not in agreement, we commenced the present investigation to determine what change the eutectoid-transformation of (β) in aluminium and zinc alloys would undergo in the ternary system.

Fortunately after many experiments, we discovered a kind of ternary non-variant point in solid state to be called the "ternary peritectoid." As already mentioned, we published some results of these investigations in the year before last, but we realised that our diagram was still incomplete. We continued our study, until we were able to determine the equilibrium diagram as described later. Of course, our investigation was carried out independently of that of Hanson and Gayler[7].

---

(1) Op. cit.
(2) Private publication in Japan, 1925.
(3) Gaz. Chim. It., (1911) 282, (1912) 353.
(4) Zeit. Metallkunde, 10 (1919), 1.
(5) J. Inst. Metals, 1 (1920), 261.
(6) Eleventh Report to the Alloy Research Committee, (1921), 201.
(7) J. Inst. Metals, (1925), advanced paper.

MATERIALS EMPLOYED,

The alloys were made from electrolytic copper, electrolytic zinc, and aluminium of 99.6% purity.

EXPERIMENTAL METHODS.

Differential thermal analysis was chiefly employed for the observation of phenomena of solidification, and also to find the transformation in solid state ; i. e , the so-called differential heating or cooling curves were obtained by reading the difference in temperature between specimen and neutral substance, heated or cooled in a furnace, as usual, but the arrangement was slightly modified as described later.

a) Differential method used for the investigation of phenomena of solidification.

Fig. 2 shows the arrangement of the measurement. As shown in the figure, two Tammann tubes made of alundum were placed in a nichrome-wound electric furnace. In one of them the specimen and in the other the neutral body made of copper or nickel was inserted respectively, and they were heated up to a temperature about 100° C. higher than the melting point of the specimen. Then the supply of electric current in the furnace was cut off, and with cooling the difference in temperature between the specimen and the neutral body was read with the deflection of a Leeds and Northrup mirror galvanometer connected to differential couple D. C. Also the temperature of the specimen was measured at the same time with a platinum platinum-rhodium thermo-couple T. C. Thus we obtained the differential cooling curves, which showed the phenomena of solidification with much sensitiveness.

Fig. 2.

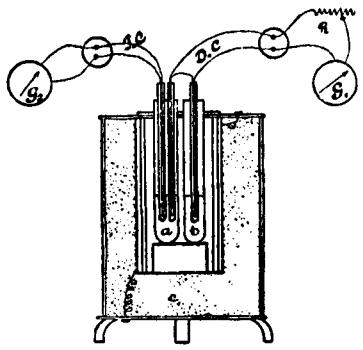

In the figure, R shows a rheostat of high resistance, which regulates the deflection of the mirror galvanometer G_1 not to be out of the scale of the telescope during measurement. In our experiment a resistance of 100 ohms was sufficient for this purpose.

As is well known, the specific gravity of aluminium is very different from that of copper and zinc. It was necessary to take specimens of the same volume, in spite of the same weight as usually employed. Therefore we prepared the specimens previously in a cylindrical form of about 40 mm. in length, and about 13 mm. in diameter, and they were melted again in the experiment.

The rate of cooling was about 5° C. per minute in the range of the temperature during which our experiment was carried out, and the deflections of the galvanometer were read each 20 seconds.

b) Differential method used for the investigation of the transformation in solids.

For this purpose a specimen 25 mm. long and 10 mm. in diameter was inserted in a cylindrical piece of aluminium, through which a hole was bored to hold the specimen, as shown in Fig. 3. They were placed in an electric furnace, and both during heating and cooling, the temperature of the specimen and the difference in temperature between the specimen and the aluminium cylinder were read similarly as above described. This method, therefore, was not different from those which had been commonly used.

Fig. 3.

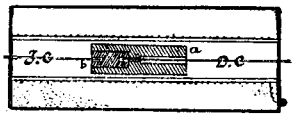

c) Measurement of thermal expansion.

Test specimens 15 cm. long and 6.5 mm. in diameter were prepared and the change of thermal expansion on heating was observed with a Honda's dilatometer. Heating was carried out at the rate of 1° C. per minute. Thus the change of solid solubility was determined.

d) Microscopical study.

For the microscopical study a piece of specimen, which had been chill-cast or heat-treated suitably, was taken and polished by hand on emery paper of grades 0,00,000. Finally it was finished on a flannel, using calcined magnesia as polishing powder. Then we developed the figure chiefly with a solution of sodium picrate, or sometimes with a solution of sodium hydroxide.

RESULTS OF EXPERIMENTS.

a) The Investigation of Phenomena of Solidification.

Measurements were made for the alloys corresponding to the compositions in the 9 kinds of constitutional sections, 8 kinds of them being taken as the section through zinc axis.

The results of experiments are given in Tables 3 to 11, and they are plotted in Figs. 4 to 12.

Table 3.

Thermal analyses of the *CZA* Series.

No.	Composition (by analysis)			Points of Change or Arrest.			
	Cu %	Zn %	Al %	°C.			
CZA 1	0.30	94.95	remainder	382	379		
„ 2	0.45	90.00	„	425	379		
„ 3	0.69	85.46	„	448	379		
„ 4	0.84	79.88	„	467	379		
„ 5	1.00	74.48	„	495	378		
„ 6	1.29	71.40	„	518	451	378	
„ 7	1.44	61.78	„	542	523	447	379
„ 8	2.08	52.97	„	569	537	447	
„ 9	2.33	43.50	„	588	538	455	
„ 10	2.72	30.45	„	615	538	457	
„ 11	3.34	21.63	„	627	559	465	
„ 12	3.76	10.93	„	644	573	494	
„ 13	4.16	—	„	651	583	545	

Table 4.
Thermal Analyses of the *CZB* Series.

No.		Composition (by analysis)			Points of Change or Arrest.			
		Cu %	Zn %	Al %	°C.			
CZB	1	0.35	96.64	remainder	402	384		
,,	2	0.55	95.16	,,	390	385		
,,	3	1.14	89.75	,,	418	407	386	
,,	4	1 66	85.91	,,	434	414	384	
,,	5	1.83	83.25	,,	444	426	384	
,,	6	2.13	79.68	,,	460		384	
,,	7	3.17	70.22	,,	482	442	392	382
,,	8	3.76	64.74	,,	504	433	394	
,,	9	4.31	60.74	,,	516	434	401	
,,	10	4.65	55.44	,,	527	420	404	
,,	11	5.25	49.99	,,	544	506	442	396
,,	12	6.44	41.83	,,	570	506	441	
,,	13	7.35	30.48	,,	602	511	460	
,,	14	8.71	20.76	,,	609	539	474	
,,	15	9.71	16.43	,,	621	548	510	
,,	16	11.53	—	,,	636	580	547	

Table 5.
Thermal Analyses of the *CZC* Series.

No.		Composition (by analysis)			Points of Change or Arrest.			
		Cu %	Zn %	Al %	°C.			
CZC	1	0.55	97.13	remainder	410	377		
,,	2	0.96	94.88	,,	387	377		
,,	3	1.93	90.63	,,	403	376		
,,	4	2.62	85.88	,,	416	375		
,,	5	3.86	80.13	,,	441	383	376	
,,	6	4.16	79.25	,,	451	387	378	
,,	7	5.84	71.63	,,	473	436	400	
,,	8	7.87	61.00	,,	505	421	411	393
,,	9	8.59	52.83	,,	524	427	397	
,,	10	10.84	47.33	,,	541	453	431	
,,	11	11.63	42.50	,,	545	451		
,,	12	13.46	34.88	,,	577	525	465	
,,	13	15.59	22.50	,,	595	541	499	
,,	14	18.07	10.88	,,	604	555	523	
,,	15	19.45	—	,,	608	547		

Table 6.

Thermal Analyses of the *CZD* Series.

No.		Composition (by analysis).			Points of Change or Arrest.				
		Cu %	Zn %	Al %	°C.				
CZD	1	1.49	95.54	remainder	401	396	381		
„	2	2.89	89.47	„	392	381			
„	3	4.51	84.52	„	415	394	381		
„	4	5.97	79.61	„	427	396	381		
„	5	7.38	74.75	„	438	401	381		
„	6	8.96	70.03	„	447	425	405		
„	7	10.40	65.95	„	453	412	395		
„	8	11.93	60.51	„	465	423	401		
„	9	14.70	51.48	„	491	443	401		
„	10	18.12	41.52	„	505	455	429	395	
„	11	20.69	30.44	„	526	482			
„	12	23.57	20.08	„	545	504			
„	13	26.67	10.02	„	564	525			
„	14	29.21	—	„	564	546			

Table 7.

Thermal Analyses of the *CZE* Series.

No.		Composition (by analysis).			Points of Change or Arrest.				
		Cu %	Zn %	Al %	°C.				
CZE	1	2.05	94.81	remainder	398	378			
„	2	4.29	89.25	„	400	383	378		
„	3	6.52	85.08	„	394	378			
„	4	7.33	79.75	„	408	392	378		
„	5	8.96	75.86	„	427	398			
„	6	11.01	69.67	„	430	410	400		
„	7	18.62	50.88	„	463	440	402		
„	8	21.28	43.50	„	476	440	401		
„	9	23.03	39.25	„	483	438	396		
„	10	24.89	31.56	„	498	480	452	425	398
„	11	29.69	21.90	„	525	507			
„	12	32.44	11.01	„	550	523			
„	13	37.50	—	„	570	549			

Table 8.

Thermal Analyses of the *CZF* Series.

No.		Composition (by analysis).			Points of Change or Arrest.				
		Cu %	Zn %	Al %	°C.				
CZF	1	2.08	95.25	remainder	403	395	379		
„	2	4.75	90.38	„	410	389	378		
„	3	6.82	85.38	„	413	391	379		
„	4	8.95	80.25	„	409	398	375		
„	5	10.94	75.50	„	424	402	379		
„	6	16.01	65.75	„	443	419	397		
„	7	17.88	62.75	„	461	417	399		
„	8	19.37	52.55	„	480	445	418	399	
„	9	27.10	42.38	„	501	451	415	399	
„	10	30.83	31.50	„	538	475			
„	11	35.32	22.31	„	543	485			
„	12	39.42	12.13	„	560	511			
„	13	44.26	—	„	584	547			

Table 9.

Thermal Analyses of the *CZG* Series.

No.		Composition (by analysis).			Points of Change or Arrest.				
		Cu %	Zn %	Al %	°C.				
CZG	1	2.35	95.15	remainder	409		376		
„	2	4.75	89.88	„	424	381	375		
„	3	7.33	84.75	„	442	390	379		
„	4	10.35	78.85	„	452	414	398	375	
„	5	12.62	75.00	„	455	399	375		
„	6	14.99	71.63	„	459	414	397		
„	7	19.31	62.50	„	471	411	397		
„	8	20.19	60.63	„	485	413	397		
„	9	23.96	53.75	„	511	447	420	397	
„	10	29.06	39.50	„	539	469	453	421	399
„	11	34.25	30.05	„	546	495	439	399	
„	12	39.45	21.13	„	551	533	443	414	
„	13	44.25	11.25	„	576	481			
„	14	50.05	—	„	596	547			

Table 10.

Thermal Analyses of the *CZH* Series.

No.	Composition (by analysis).			Points of Change or Arrest.			
	Cu %	Zn %	Al %	°C.			
CZH 1	5.96	90.67	remainder	454	388	381	
„ 2	11.72	80.05	„	480	402	383	
„ 3	17.63	69.44	„	496	428	404	
„ 4	24.40	60.06	„	532	416	404	
„ 5	29.72	49.50	„	560	430	404	
„ 6	34.39	42.77	„	588	444	420	404
„ 7	42.74	30.06	„	604	436	417	403
" 8	48.31	20.73	„	641	492		
„ 9	50.69	15 48	„	640	530		
„ 10	53.66	10.17	„	648	594	554	
„ 11	56.43	5.26	„	654			
„ 12	60.19	—	„	649	624	590	

Table 11.

Thermal Analyses of the *CZI* Series.

No.	Composition (by analysis).			Points of Change or Arrest.		
	Cu %	Zn %	Al %	°C.		
CZI 1	16.78	remainder	—	681	593	
„ 2	18.12	77.96	remainder	650	591	382
„ 3	19.45	73.76	„	638	590	399
„ 4	20.64	71.65	„	631	587	401
„ 5	22.77	65.71	„	587	440	401
„ 6	24.65	61.13	„	593	401	
„ 7	26.66	56.18	„	575	416	401
„ 8	30.05	49.50	„	565	433	401
„ 9	45.65	10.03	„	574	560	415
„ 10	50.05	—	„	596	547	

Fig. 4. CZA Series.

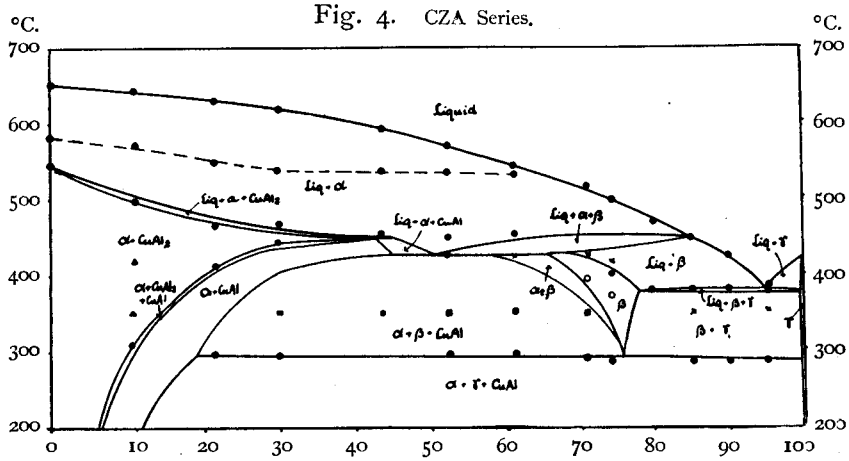

Fig. 5. CZB Series.

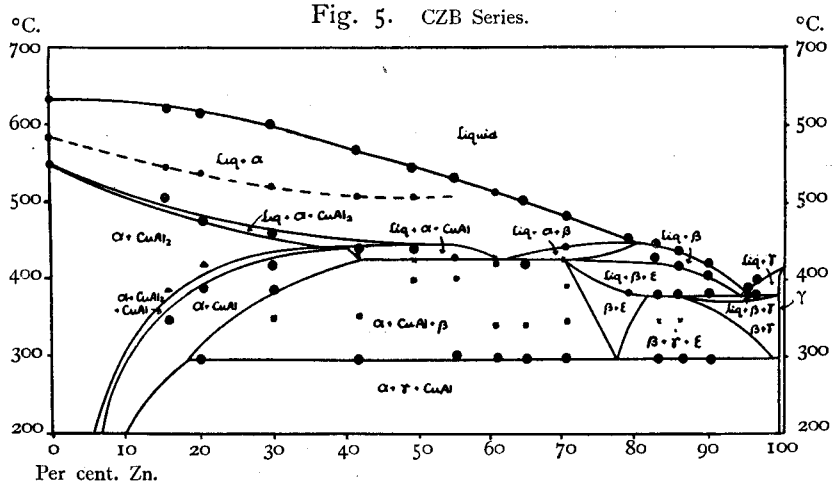

Fig. 6. CZC Series.

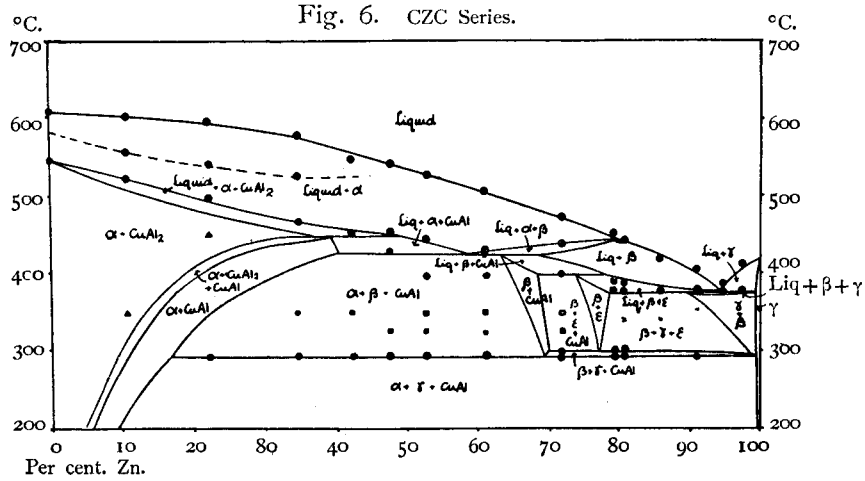

Fig. 7. CZD Series.

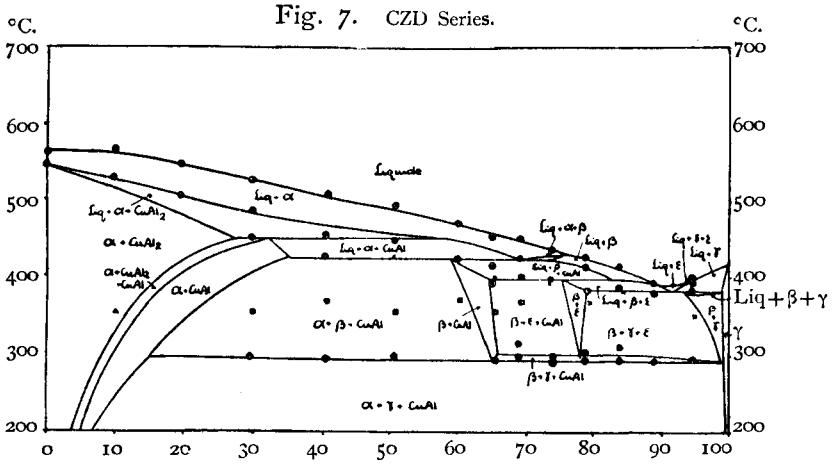

Fig. 8. CZE Series.

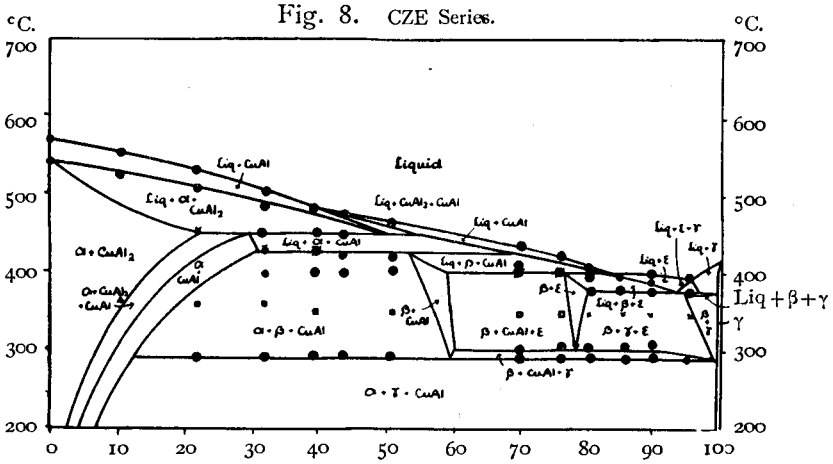

Fig. 9. CZF Series.

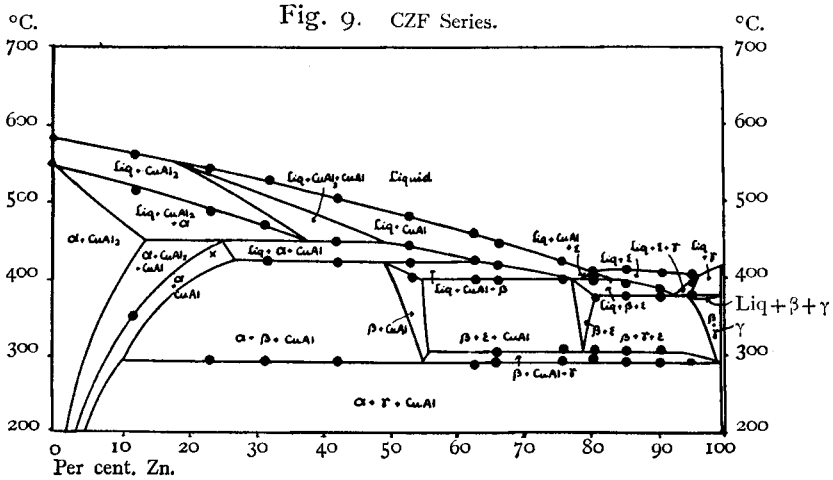

Fig. 10. CZG Series.

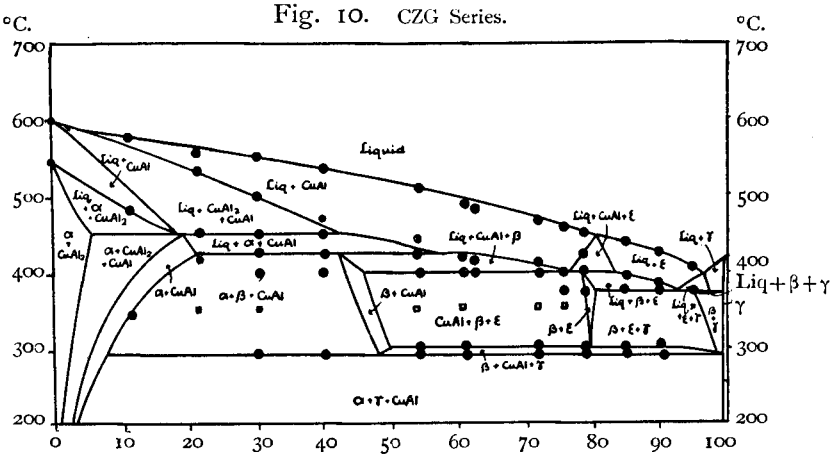

Fig. 11. CZH Series.

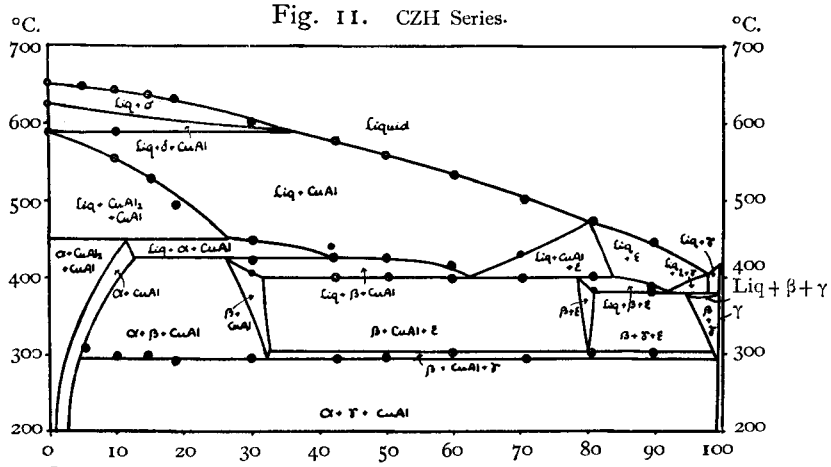

Fig. 12. CZI Series.

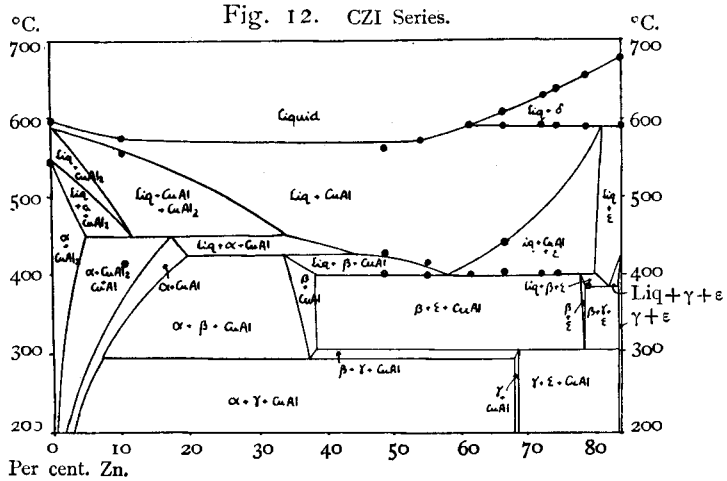

From these results we observed not only the points of arrest at 385° C. and 425° C., but also a new halting point at 450° C. in the alloys of the *A* and the *B* series, as shown in Figs. 4 and 5. As explained later, this invariant halting at 450° C. was found to be a peritecto-eutectic reaction.

$$\text{liquid} + CuAl_2 \rightleftarrows (\alpha) + CuAl,$$

in which (α) denotes the aluminium-rich solid solution. We did not find it in the results given by Jareš, Hanson and Gayler, but its existence was proved more distinctly in the alloys of the other sections.

The evolution of heat at 580° C. in the aluminium-copper alloys was also observed in the alloys of aluminium, copper, and zinc, but the temperature was gradually depressed by the addition of zinc, until it became almost constant. Therefore it must be ascribed to the transformation of a certain property in the aluminium-rich solid solution, but we could not determine to what property it had to be attributed. Perhaps it might be such a transformation as the β change in iron.

Similarly, as given by Jareš and Hanson, the points of arrest at 425° C., 400° C., and 385° C. were observed. They belong to the invariant reactions

$$\text{liquid} + (\alpha) \rightleftarrows CuAl + (\beta),$$
$$\text{liquid} + CuAl \rightleftarrows (\beta) + (\varepsilon),$$
and
$$\text{liquid} + (\varepsilon) \rightleftarrows (\beta) + (\gamma),$$

in which we denote the solid solution in aluminium-zinc alloys as (β), the solid solution corresponding to $CuZn_4$ as (ε), and the solid solution rich in zinc as (γ).

In our experiments, cooling was not very slow, in order that the equilibrium might be attained at any instant. Consequently, some alloys, such as *CZA* 5, 6, and 7, showed markedly the phenomena of super-cooling and gave signs of halting at 385° C., which had to disappear, if equilibrium was to be attained. Moreover, super-cooling often caused invariant haltings to occur at lower temperatures. In the alloys of the other sections such phenomena were also observed, but their non-existence or the true

temperature was confirmed microscopically or with heating curves after annealing.

In addition to the invariant arrests above mentioned, we found an invariant arrest at 590° C., which is given by Jareš as denoting the reaction

$$\text{liquid} + (\delta) \rightleftarrows CuAl + (\varepsilon).$$

Thus we observed 5 invariant haltings at 380° C., 400° C., 425° C., 450° C., and 590° C. in the alloys of our experiments.

As is well known, the observation on cooling at the ordinary rate is not sufficient to determine the constitution in equilibrium, as the cooling is not so slow that it gives rise to the so-called super-cooling, hence it does not give us the phenomena of solidification in equilibrium immediately. Therefore, the temperatures of the beginning of melting were determined on heating curves obtained similarly with differential method, using the same specimens as were employed for the study of solid transformation.

The results of the measurements are given in Table 12.

Table 12.

The Beginning of Melting.

No.	Composition (by analysis).			Temperature of the Beginning of Melting.
	Cu %	Zn %	Al %	°C.
CZA 1	0.30	94.95	remainder	387
„ 4	0.84	79.88	„	387
„ 5	1.00	74.48	„	414
„ 6	1.29	71.40	„	428
„ 7	1.44	61.78	„	424
„ 8	2.08	52 97	„	424
„ 11	3.34	21.63	„	469
CZB 3	1.14	89.75	„	385
„ 4	1.66	85.91	„	385
„ 7	3.17	70.22	„	425
„ 8	3.76	64.74	„	424
„ 9	4.31	60.74	„	430
„ 10	4.65	55.44	„	428
„ 11	5.25	49.99	„	425

No.	Composition (by analysis).			Temperature of the Beginning of Melting.
	Cu %	Zn %	Al %	°C.
CZB 12	6.44	41.83	remainder	436
CZC 1	0.55	97.13	,,	384
,, 4	2 62	85.88	,,	386
,, 8	7.87	61.00	,,	424
CZD 1	1.49	95.54	,,	386
,, 3	4.51	84.53	,,	387
,, 5	7.38	74.75	,,	396
,, 4	5 97	79.61	,,	386
,, 6	8.96	70.03	,,	406
,, 7	10.40	65.95	,,	408
,, 9	14.70	51.48	,,	429
,, 10	18.12	41.53	,,	428
CZE 1	2.06	94.81	,,	388
,, 2	4.29	89.25	,,	387
,, 4	7.33	79.75	,,	387
,, 5	8.95	75.86	,,	402
,, 6	11.01	69.69	,,	406
,, 8	21.28	43.50	,,	422
,, 9	23.03	39.25	,,	427
,, 10	24.89	31.56	,,	431
,, 11	29.63	21.90	,,	451
CZF 2	4.75	90.38	,,	384
,, 4	8.94	80.25	,,	387
,, 5	10.94	75.50	,,	396
,, 6	16.01	65.75	,,	404
,, 10	30.83	31.50	,,	423
,, 11	35.32	22.31	,,	432
CZG 2	4.75	89.88	,,	385
,, 4	10.35	78.85	,,	397
,, 6	14.99	71.63	,,	404
,, 8	20.19	60.63	,,	407
,, 9	23.96	53.75	,,	404
,, 11	34.25	30.05	,,	424
Al-Zn	—	5.00	,,	381

From the results of these thermal analyses of heating it was confirmed that the non-variant reaction observed at 380° C. on cooling occurred at a

somewhat higher temperature on heating, compared with the binary eutectic point 380° C. in aluminium-zinc alloys. Consequently the invariant arrest must be represented by the peritecto-eutectic reaction

$$\text{liquid} + (\varepsilon) \rightleftarrows (\beta) + (\gamma).$$

In summarizing these thermal analyses of heating and cooling, we conclude that the reaction

$$\text{liquid} + CuAl_2 \rightleftarrows CuAl + (\beta)$$

at 418° C. given by Jareš and others did not appear in our experiment, but on the other hand a new peritecto-eutectic reaction

$$\text{liquid} + CuAl_2 \rightleftarrows CuAl + (\alpha)$$

was determined to exist at the temperature 450° C.

The other non-variant reactions

$$\text{liquid} + (\alpha) \rightleftarrows (\beta) + CuAl$$

and

$$\text{liquid} + CuAl \rightleftarrows (\beta) + (\varepsilon)$$

were similarly observed as in the previous investigations.

According to the experiments above mentioned, the phenomena of solidification were for the most part manifested. But the aluminium-rich alloys of aluminium, copper, and zinc are most important in industry; hence our experiments were still aimed at investigating in detail the constitution of them. For the purpose, thermal curves on cooling were similarly taken of series of the aluminium-rich alloys in 6 sections representing the constant content of copper, and the temperatures of liquidus points were determined. The solidus points, however, were obtained with thermal analyses on heating. The results of experiments are summarized in Table 13, and they are plotted in Figs. 13 to 18.

From the results obtained on cooling curves we see that the most of alloys except those containing 1 and 2 per cent. of copper showed 3 thermal changes. The highest one corresponds evidently to the beginning of solidification, and the second represents the thermal change corresponding

Fig. 13.

ZA Series.

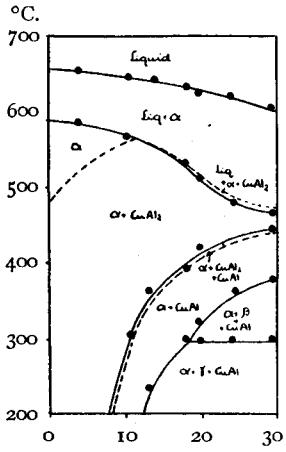

Per cent. Zn.

Fig. 14.

ZB Series.

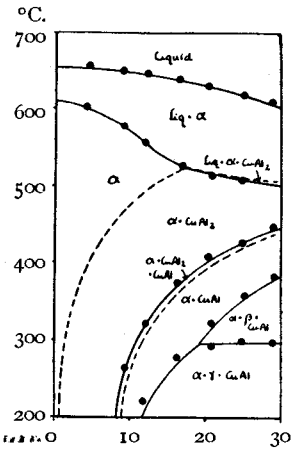

Per cent. Zn.

Fig. 15.

ZC Series.

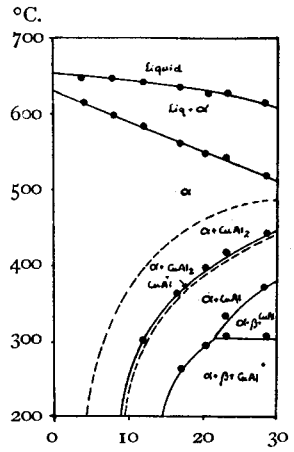

Per cent. Zn.

Fig. 16.

ZD Series.

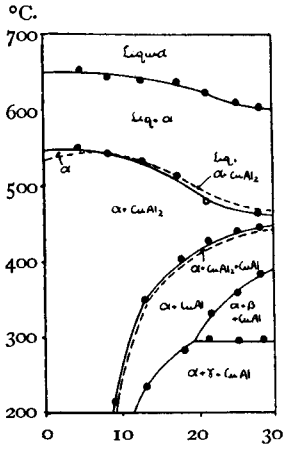

Per cent. Zn.

Fig. 17.

ZE Series.

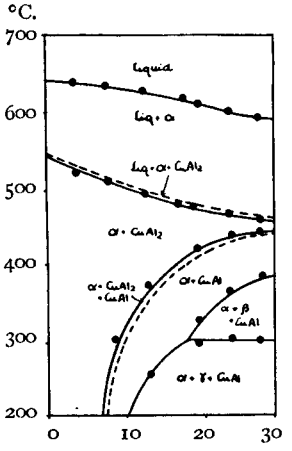

Per cent. Zn.

Fig. 18.

ZF Series.

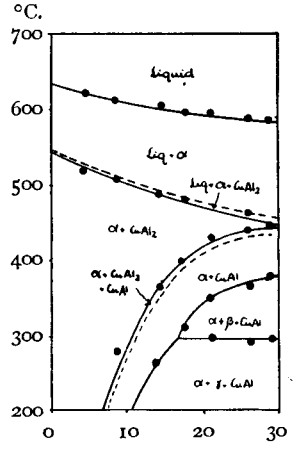

Per cent. Zn.

Table 13.

Thermal Analyses of Aluminium-rich Alloys in 6 Sections representing the Constant Content of Copper.

No.		Composition (by analysis).			Points of Change or Arrest. °C.			
		Cu %	Zn %	Al %	on Cooling			on Heating
ZA	1	1.02	3.97	remainder	649			614
„	2	1.58	7.94	„	647			597
„	3	1.57	12.06	„	639			585
„	4	1.09	16.91	„	634			557
„	5	1.04	20.34	„	628			549
„	6	1.08	22.88	„	622			539
„	7	0.97	28.13	„	618.			516
ZB	1	2.05	4.46	remainder	654			610
„	2	2.15	8.97	„	644		488	578
„	3	2.28	11.86	„	635		467	558
„	4	1.98	16.76	„	631		463	519
„	5	2.33	20.43	„	629		456	510
„	6	2.10	24.51	„	617		458	508
„	7	1.92	28.67	„	609		458	—
ZC	1	3.23	4.21	remainder	652	(578)	520	584
„	2	3.22	10.58	„	647	(548)	500	565
„	3	3.02	13.33	„	640	(554)	486	—
„	4	3.41	18.38	„	628	(546)	457	483
„	5	3.14	19.83	„	621	(544)	450	479
„	6	3.46	24.26	„	620	(538)	450	473
„	7	3.37	29.89	„	604	(524)	453	465
ZD	1	4.74	4.41	remainder	648	(571)	512	575
„	2	4.55	8.72	„	647	(570)	508	552
„	3	4.98	13.03	„	640	(552)	492	510
„	4	4.99	17.64	„	639	(544)	481	490
„	5	4.68	21.03	„	623	(523)	450	468
„	6	4.63	25.33	„	607	(519)	440	—
„	7	4.83	28.18	„	605	(518)	450	461
ZE	1	7.65	4.12	remainder	638	(568)	526	567

No.	Composition (by analysis).			Points of Change or Arrest. °C.			
	Cu %	Zn %	Al %	on Cooling			on Heating
ZE 2	7.38	8.58	remainder	629	(548)	508	513
„ 3	7.46	13 38	„	627	(540)	495	501
„ 4	7.67	18.38	„	622	(522)	468	480
„ 5	7.23	19.84	„	608	(512)	470	475
„ 6	7.57	24.86	„	594	(508)	460	460
„ 7	7.28	28.42	„	594	(508)	450	460
ZF 1	9.92	4.17	remainder	624	(548)	521	516
„ 2	9.90	8.48	„	615	(538)	506	510
„ 3	10.09	14.46	„	606	(518)	485	493
„ 4	10.04	17.30	„	597	(510)	485	483
„ 5	10.28	20.62	„	598	(510)	473	—
„ 6	9.97	25.73	„	593	(512)	465	468
„ 7	9.60	28.52	„	587	(510)	457	457

to the evolution of heat at 580° C. in the binary alloys of aluminium and copper. In the table they are given in parenthesis. The third one indicates a binary reaction

$$\text{liquid} \rightarrow (\alpha) + CuAl_2$$

has commenced at this temperature.

b) The study of Solid Transformation.

The specimens which had been previously annealed at 350° C. were once more heated at about 170° C. for 10 days in an automatic regulating electric air bath. This prolonged heating was necessary to bring them completely into the state of lower temperatures. Then we obtained the heating and cooling curves with the differential method already mentioned. The rate of heating and cooling was about 3° C. per minute. The results of the experiments are given in Tables 14 to 21 inclusive, and they are also plotted in the constitutional sections as shown in Figs. 4 to 12.

Table 14.

Thermal Analyses of the *CZA* Series in Solids.

No.	Composition (by analysis).			The Temperature of Transformation.	
	Cu %	Zn %	Al %	on Heating.	on Cooling.
CZA 1	0.30	94.95	remainder	284	261
„ 3	0.69	85.46	„	284	—
„ 5	1.00	74.48	„	283	255
„ 6	1.29	71.40	„	292	259
„ 7	1.44	61.78	„	295	246
„ 9	2.72	30.45	„	294	—
„ 10	3.34	21.63	„	294	250
„ 11	3.76	10.93	„	295	255

Table 15.

Thermal Analyses of the *CZB* Series in Solids.

No.	Composition (by analysis).			The Temperature of Transformation.	
	Cu %	Zn %	Al %	on Heating.	on Cooling.
ZCB 3	1.14	89.75	remainder	293	258
„ 4	1.66	85.91	„	294	272
„ 5	1.83	83.25	„	293	272
„ 7	3.17	70.22	„	294	267
„ 8	3.76	64.74	„	293	264
„ 9	4.31	60.74	„	302	254
„ 10	4.65	55.44	„	300	260
„ 12	6.44	41.83	„	301	252
„ 14	8.71	20.67	„	300	—

Table 16.

Thermal Analyses of the *CZC* Series in Solids.

No.	Composition (by analysis).			The Temperature of Transformation.	
	Cu %	Zn %	Al %	on Heating,	on Cooling.
CZC 3	1.93	90.63	remainder	294 —	265
„ 5	3.86	80.13	„	295 314	260
„ 6	4.16	79.25	„	294 310	258
„ 7	5.84	71.63	„	288 294	265
„ 8	7.87	61.00	„	288 —	256
„ 9	8.59	52.83	„	288 —	252
„ 10	10.84	47.33	„	292 —	—
„ 11	11.63	42.50	„	292 —	248
„ 12	13.46	34.88	„	293 —	268
„ 13	15.59	22.50	„	294 —	250

Table 17.

Thermal Analyses of the *CZD* Series in Solids.

No.	Composition (by analysis).			The Temperature of Transformation.	
	Cu %	Zn %	Al %	on Heating.	on Cooling.
CZD 1	1.49	95.54	remainder	290 —	268 —
„ 2	2.89	89.47	„	292 —	269 —
„ 3	4.51	84.52	„	301 312	252 —
„ 4	5.97	79.61	„	295 304	258 —
„ 5	7.38	74.75	„	290 298	296 269
„ 6	8.96	70.03	„	299 314	252 —
„ 7	10.39	65.95	„	290 —	262 —
„ 9	14.70	51.48	„	299 —	252 —
„ 10	18.12	41.52	„	293 —	252 —
„ 11	20.69	30.44	„	292 —	240 —

Table 18.

Thermal Analyses of the *CZE* Series in Solids.

No.	Composition (by analysis).			The Temperature of Transformation.	
	Cu %	Zn %	Al %	on Heating.	on Cooling.
CZE 1	2.06	94.81	remainder	292 —	264 —
„ 2	4.29	89.25	„	294 312	264 —
„ 3	6.52	85.08	„	294 304	266 —
„ 4	7.33	79.75	„	294 304	256 —
„ 5	8.95	75.86	„	294 306	286 264
„ 6	11.01	69.67	„	294 304	272 257
„ 7	18.62	50.88	„	294 —	252 —
„ 8	21.22	43.50	„	294 —	254 —
„ 9	23.08	39.25	„	294 —	246 —
„ 10	24.89	31.56	„	292 —	— —
„ 11	29.69	21.90	„	294 —	— —

Table 19.

Thermal Analyses of the *CZF* Series in Solids.

No.	Composition (by analysis).			The Temperature of Transformation.	
	Cu %	Zn %	Al %	on Heating.	on Cooling.
CZF 1	2.08	95.25	remainder	290 —	265 —
„ 2	4.75	90.38	„	298 313	260 —
„ 3	6.82	85.38	„	293 308	260 —
„ 4	8.94	80.25	„	300 313	264 252
„ 5	10.94	75.50	„	300 308	279 254
„ 6	16.01	65.75	„	292 304	262 252
„ 7	17.89	62.75	„	290 —	266 260
„ 9	27.10	42.38	„	296 —	250 —
„ 10	30.83	31.50	„	294 —	250 —
„ 11	35.32	22.31	„	300 —	240 —

Table 20.
Thermal Analyses of the *CZG* Series in Solids.

No.	Composition (by analysis).			The Temperature of Transformation.	
	Cu %	Zn %	Al %	on Heating.	on Cooling.
CZG 2	4.75	89.88	remainder	301 310	265 —
„ 3	7.33	84.75	„	292 306	268 —
„ 4	10.35	78.85	„	296 308	287 260
„ 6	14.99	71.63	„	298 308	280 242
„ 8	20.19	60.63	„	292 306	270 254
„ 9	23.96	53.75	„	291 302	260 250
„ 10	29.06	39.50	„	294 —	252 —
„ 11	34.05	30.05	„	297 —	251 —

Table 21.
Thermal Analyses of the *CZH* Series in Solids.

No.	Composition (by analysis).			The Temperature of Transformation.	
	Cu %	Zn %	Al %	on Heating.	on Cooling.
CZH 1	5.96	90.67	remainder	303	267
„ 2	11.72	80.05	„	300	261
„ 3	17.64	69.44	„	298	260
„ 4	24.40	60.06	„	302	258
„ 5	29.72	49.50	„	292	258
„ 6	34.39	42.77	„	292	258
„ 7	42.74	30.06	„	292	252
„ 8	48.31	20.73	„	290	252
„ 9	50.69	15.48	„	298	245
„ 10	53.66	10.17	„	297	—
„ 11	56.43	5.26	„	312	—

In the alloys of the *CZA* Series containing more than 75 per cent. of zinc, an absorption of heat was observed at 284° C. on heating, and a similar reaction was also found at 292° C. in the alloys containing zinc less than the former, as shown in these results of our experiments. Also we observed the same transformation at 292° C. in the alloys of the section *B*.

On the other hand, such transformation was found to occur in 2 steps at 292° C. and 303° C. on heating in some of the alloys in the other

sections. Sometimes these absorptions of heat overlapped and the reaction at 303° C. was noticed at a somewhat higher temperature.

In general, the measurements on cooling gave irregular results and they did not indicate the transformation in 2 steps so distinctly as on heating. Therefore we adopted the temperature on heating in the diagram.

The eutectoid transformation of (β) in the binary alloys of aluminium and zinc is known to occur at 280° C. on heating and at 260° C. on cooling. However, the solid transformation is generally much suppressed on cooling, hence the temperature given by the heating curve indicates rather the temperature true or close to the transformation in equilibrium. Furthermore, it is evident from the fact that in the alloys of aluminium, zinc, and tin[1] the reaction

$$\text{liquid} + (\beta) \rightleftarrows (\alpha) + (\gamma)$$

occurs at 280° C. on cooling. This illustrates the fact that the eutectoid transformation of (β) in the alloys of aluminium and zinc takes place at 280° C. even on cooling, if the reaction proceeds without suppression. From these considerations we adopted the temperature on heating.

As the transformations in the alloys of aluminium, zinc, and copper take place at temperatures higher than the eutectoid in aluminium and zinc alloys, none of them can be thought to be a ternary eutectoid, but they must be attributed to such invariant reactions as

$$(\beta) + (\varepsilon) \rightleftarrows (CuAl) + (\gamma) \text{ at } 303° \text{ C.},$$

and

$$(\beta) + (CuAl) \rightleftarrows (\alpha) + (\gamma) \text{ at } 292° \text{ C.}$$

However, they cannot be said to be due to such reactions as

$$(\beta) + CuAl_2 \rightleftarrows CuAl + (Al) \text{ at } 270°\text{C.},$$

and

$$(\beta) + CuZn_4 \rightleftarrows CuAl + (Zn) \text{ at } 265° \text{ C.},$$

as given by Hanson and Gayler. Because we recognized the reaction at 450° C. and not the reaction at 418° C. Moreover, the thermal analyses did not show the transformation in 2 steps in the whole range

(1) The writer; J. Mining and Metallurgy, Kyoto, 4 (1925), 1441.

of the compositions given by Hanson and Gayler, but only in some zinc-rich part. We see also in the diagram of Hanson that an alloy containing 10 per cent. of copper and 70 per cent. of zinc shows the transformation in one step; but in our experiments such alloys as *CZD* 6 and 7 indicated clearly the change in 2 steps. From these standpoints we can say that the solid transformations in 2 steps must be due to the reactions above mentioned.

At all events, both of them belong to the "ternary eutecto-peritectoid" (for simplicity we say "ternary peritectoid"), as the writer has often published, in Japan, the existence of such a solid transformation.

In this way the invariant reactions in solids were easily determined by means of differential thermal analysis. But thermal analysis can not be applied to determine the surfaces of solid solubility, as the change of solid solubility is a reaction which takes place gradually and does not accompany any distinct thermal effect. For the purpose, therefore, we have no other means to rely upon than microscopical study or the measurement of such physical properties as specific volume or electric resistivity. In our experiments, thermal expansion was measured of alloys, whose content of copper varied from 1 to 10 per cent., and whose content of zinc varied from 4 to 28 per cent., and we determined the surfaces of solid solubility in the aluminium rich alloys.

Table 22

Measurement of the Thermal Expansion of Aluminium-rich Alloys.

No.	Composition (by analysis).			Points of Transformation.		
	Cu %	Zn %	Al %	°C.		
ZA 1	1.02	3.97	remainder	—		
„ 2	1.58	7.94	„	—		
„ 3	1.57	12.06	„	300		
„ 4	1.09	16.91	„	264	361	
„ 5	1.04	20.34	„	287	403	
„ 6	1.08	22.88	„	307	333	417
„ 7	0.97	28.13	„	310	373	443

No.		Composition (by analysis).			Points of Transformation.		
		Cu %	Zn %	Al %	°C.		
ZB	1	2.05	4.46	remainder	—		
,,	2	2.15	8.97	,,	263		
,,	3	2.28	11.86	,,	220	321	
,,	4	1.98	16.76	,,	277	370	
,,	5	2.33	20.43	,,	294	324	412
,,	6	2.10	24.51	,,	294	358	430
,,	7	1.92	28.67	,,	296	385	443
ZC	1	3.23	4.21	remainder	—		
,,	2	3.22	10.54	,,	302		
,,	3	3.02	13.33	,,	236	362	
,,	4	3.42	18.38	,,	298	394	
,,	5	3.14	19.83	,,	292	323	422
,,	6	3.46	24.26	,,	302	366	
,,	7	3.37	29.89	,,	302	379	432
ZD	1	4.74	4.41	remainder	—		
,,	2	4.55	8.72	,,	214		
,,	3	4.98	13.03	,,	233	348	
,,	4	4.99	17.64	,,	280	404	
,,	5	4.68	21.03	,,	295	323	428
,,	6	4.63	25.33	,,	297	357	441
,,	7	4.83	28.18	,,	294	380	445
ZE	1	7.65	4.12	remainder	—		
,,	2	7.38	8.58	,,	302		
,,	3	7.46	13.38	,,	251	375	
,,	4	7.67	18.38	,,	—		
,,	5	7.23	19.84	,,	298	330	415
,,	6	7.57	24.86	,,	301	364	442
,,	7	7.28	28.42	,,	300	375	445
ZF	1	9.92	4.17	remainder	—		
,,	2	9.90	8.48	,,	292		
,,	3	10.09	14.46	,,	264	368	
,,	4	10.49	17.30	,,	314	400	
,,	5	10.28	20.69	,,	296	357	436
,,	6	9.97	25.73	,,	295	365	443
,,	7	9.60	28.52	,,	295	380	447

The specimens employed were previously annealed at 180° C. for about one month, in order that they might attain the state of lower temperatures. The results of experiment are given in Table 22, and they are plotted in Figs. 13 to 18.

Fig. 19.

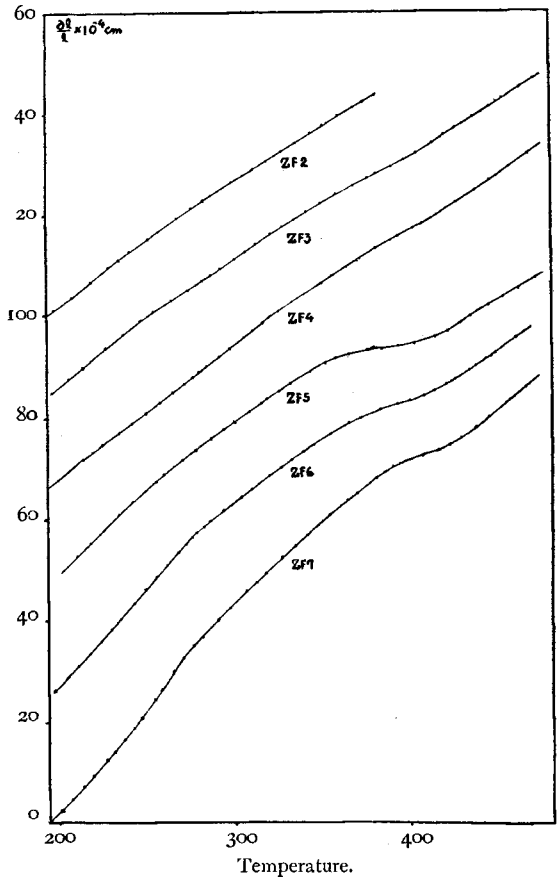

Some examples of the curves of thermal expansion are shown in Fig. 19. Among them, one typical example is represented by an alloy *ZF 7* (*Cu* 9.60%, *Zn* 28.52%). As it is evident from the results of thermal analysis, we see that such an alloys as *ZF 7* consists of (α)+(γ) + *CuAl* at room temperature, but the solubility of (γ) and *CuAl* in (α) varies with the rise of temperature. This is shown by the gradual change

of the rate of expansion on the curve of thermal expansion. The change at about 290° C. indicates that the invariant reaction

$$(\alpha)+(\gamma) \rightleftarrows (\beta)+CuAl$$

takes place and it is changed into $(\alpha)+(\beta)+CuAl$. On further heating the (β) is dissolved in (α) and then $CuAl$ is transformed into $CuAl_2$. Finally at about 447° C. it is changed into $(\alpha)+CuAl_2$. All of these transformations are also indicated by the change of expansion on the heating curves.

The other typical one is shown by an alloy *ZF* 3 (*Cu* 10.09%, *Zn* 14.46%). It consists of $(\alpha)+(\gamma)+CuAl$ at room temperature, but at about 264° C. the (γ) is entirely dissolved into (α). On further heating, the transformation $CuAl \rightarrow CuAl_2$ occurs and subsequently it is changed into $(\alpha)+CuAl_2$. These reactions are all observed on the curve of thermal expansion by the change of the rate of expansion.

In the other series of alloys we observed also similar changes of thermal expansion. In short, the former example represents the alloys whose content of zinc is more than about 18 to 20 per cent., and which show the invariant reaction

$$(\alpha)+(\gamma) \rightleftarrows (\beta)+CuAl \text{ at } 292^\circ \text{ C.},$$

and the latter represents the alloys whose content of zinc is less than about 18 to 20 per cent. and which do not show the invariant reaction above mentioned.

On cooling, these reactions to take place could not be observed owing to the so-called super-cooling ; hence heating curves were only taken to determine the temperatures of transformation as above described. Even on heating, however, the temperatures of transformation given by the present experiment would be presumably somewhat higher than those in equilibrium, because the solubility change in solid state is in general very slow, and equilibrium can be regarded not to be attained in each instant with such a rate of heating as 1° C. per min. Especially the transformation $CuAl \rightarrow CuAl_2$ was found to be the slowest one. As later described, this fact was also observed in microscopical study.

Fig. 20 shows the liquidus of the alloys obtained from the above

results, and Figs. 21 to 31 represent the constitutional sections containing the constant quantity of zinc, 10 per cent., 20 per cent., etc.

Fig. 20.

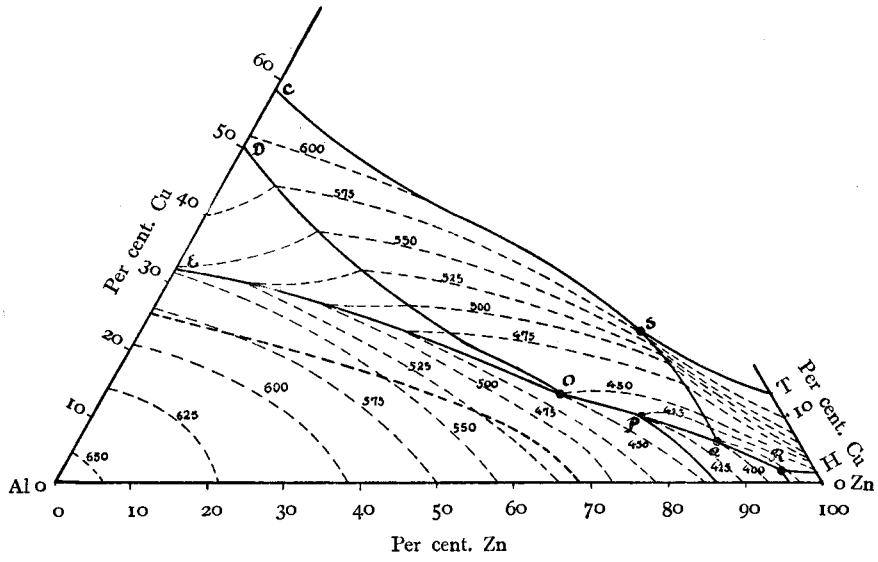

Fig. 21.

Zn 10%.

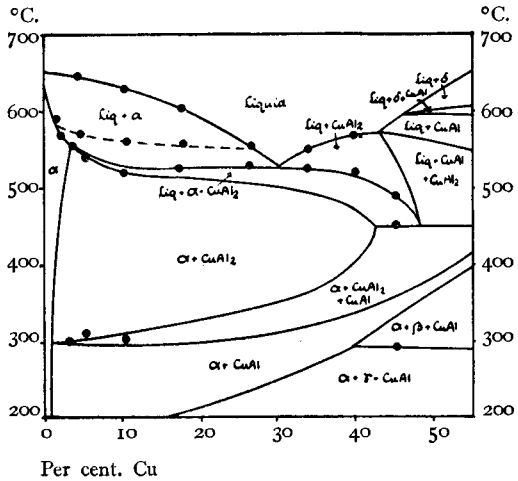

Fig. 22.

Zn 20%.

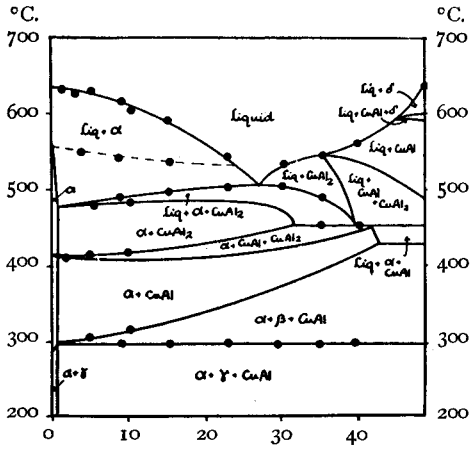

Per cent. Cu

Fig. 23.

Zn 30%.

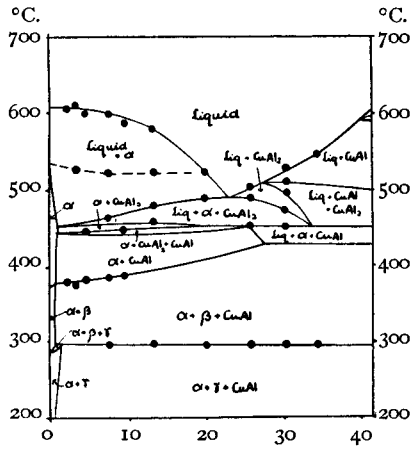

Per cent. Cu

Fig. 24.

Zn 40%.

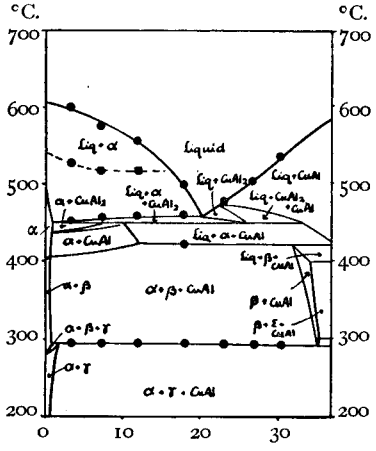

Per cent. Cu

Fig. 25.

Zn 50%.

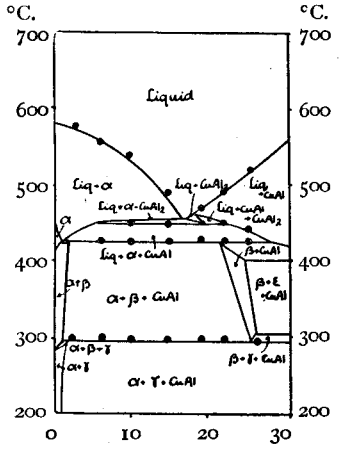

Per cent. Cu

Fig. 26.
Zn 60%.

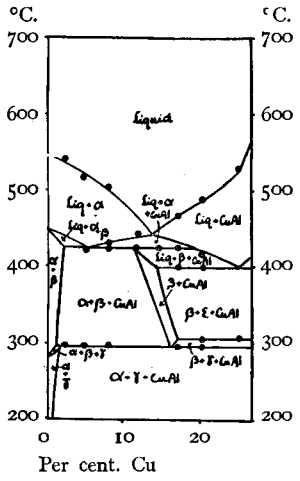

Fig. 27.
Zn 70%.

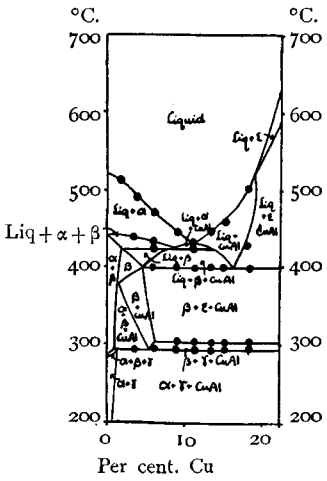

Fig. 28.
Zn 80%.

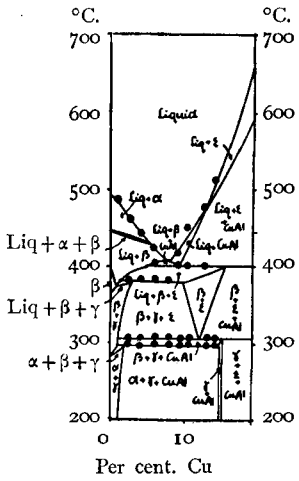

Fig. 29.
Zn 85%.

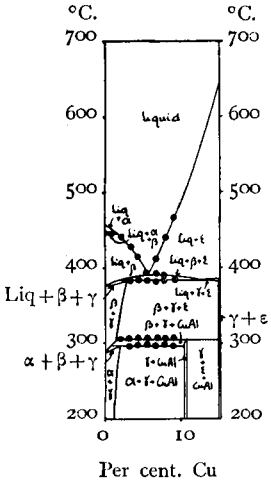

Fig. 30.
Zn 90%.

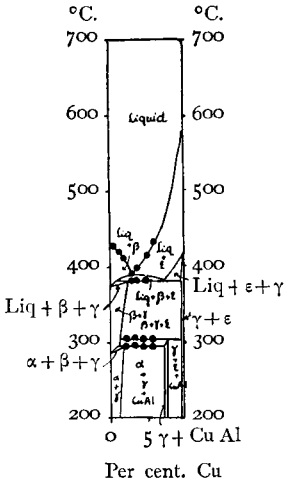

Fig. 31.
Zn 95%.

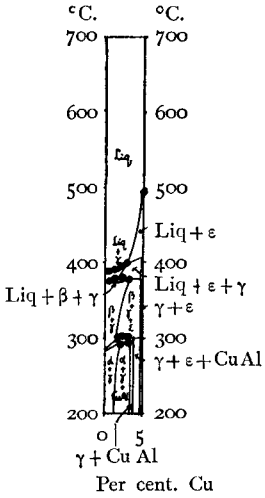

Summarizing the results of the thermal analyses for liquid and solid, we obtained the general equilibrium diagram as shown in Fig. 32. In this diagram, we denote the invariant points on the liquidus surface as O, P, Q, R, and S, and the invariant in solids as x and y. They are summarized in the following Table.

Table 23.

Invariant Points

Point.	Composition.			Temperature.	Reaction.	The Region of Reaction.
	Cu %	Zn %	Al %	°C.		
O	13.0	59.0	28.0	450	Liquid + Cu Al_2 ⇆ (α) + CuAl	KhsO
P	10.0	71.0	19.0	425	Liquid + (γ) ⇄ (β) + CuAl	KtlP
Q	5.5	84.0	10.5	400	Liquid + CuAl ⇄ (β) + (ε)	mQk_1K
R	1.5	93.0	55.5	385	Liquid + (ε) ⇄ (β) + (γ)	nRok
S	23.0	65.0	12.0	590	Liquid + (δ) ⇄ (ε) + CuAl	KSg_1
x	1.0	76.0	23.0	303	(β) + (ε) ⇄ CuAl + (γ)	$Kxjf_1$
y	0.5	75.5	24.0	292	(β) + CuAl ⇄ (α) + (γ)	Kvyw

In the diagram, we see also that the primary separation of (*α*) occurs in the region *AFPOE*, and in the region *FGRQP* the (*β*) separates primarily.

The regions of the primary separation of (*γ*), (ε), (*δ*), *CuAl*, and $CuAl_2$ are respectively represented by *BHRG*, *HISQ*, *ISCK*, *CDOPQS*, and *DEO*.

The binary complex lines showing the uni-variant reactions in these alloys are summarized in Tables 24 and 25.

These uni-variant lines in solid phases indicate that the ternary solid solution reaches its saturation of solubility for the other 2 phases along this line, e. g., from (*α*) separate $CuAl_2$ and *CuAl* along the line *su* on cooling, and on heating the reaction proceeds from the right to the left. To speak truely, this reaction is a mutual one among (*α*), $CuAl_2$ and *CuAl* to be represented by $CuAl_2 \rightleftarrows \alpha \rightleftarrows CuAl$. In this table, however, are shown only the uni-variant lines concerning the solid solutions (*α*) and (*β*), but if the other phases have their solubility in ternary alloys, there must exist such lines as shown in Fig. 32, and among them such lines as *vp* and *yq* are conjugate with each other.

Table 24.

Binary Complex Lines on Liquidus.

Binary Complex Line.	Reaction.
EO	Liquid $\rightleftarrows (\alpha) + CuAl_2$
DO	Liquid + CuAl $\rightleftarrows$ CuAl$_2$
OP	Liquid + $\rightleftarrows (\alpha) + CuAl$
FP	Liquid + $(\alpha) \rightleftarrows (\beta)$
PQ	Liquid $\rightleftarrows (\beta) + CuAl$
QR	Liquid $\rightleftarrows (\beta) + (\varepsilon)$
HR	Liquid + $(\varepsilon) \rightleftarrows (\gamma)$
RG	Liquid $\rightleftarrows (\beta) + (\gamma)$
IS	Liquid + $(\delta) \rightleftarrows (\varepsilon)$
CS	Liquid + $(\delta) \rightleftarrows$ CuAl
SQ	Liquid $\rightleftarrows$ CuAl + (ε)

Table 25.

Univariant Lines in Solid Phases.

Univariant Line.	Reaction.
su	$(\alpha) \rightleftarrows CuAl_2 + CuAl$
tv	$(\alpha) \rightleftarrows (\beta) + CuAl_2$
vp	$(\alpha) \rightleftarrows (\beta) + (\gamma)$
vz	$(\alpha) \rightleftarrows (\gamma) + CuAl$
ly	$(\beta) \rightleftarrows (\alpha) + CuAl$
mx	$(\beta) \rightleftarrows (\varepsilon) + CuAl$
nx	$(\beta) \rightleftarrows (\varepsilon) + (\gamma)$
xy	$(\beta) \rightleftarrows (\gamma) + CuAl$
yq	$(\beta) \rightleftarrows (\alpha) + (\gamma)$

MICROSCOPICAL STUDY.

For microscopical study, chill-cast or heat treated specimens were taken and some typical ones are given in Figs. 1 to 36 (Plates I to III) inclusive.

Fig. 1, under a magnification of 150 diameters, represents the microstructure of the chill cast alloy *CZA* 3 (*Cu* 0.69%, *Zn* 85.46%), in which (β) is present as black dendritic crystallites in the ground of the eutectic mixture $(\beta)+(\gamma)$, but in the alloy *CZA* 4 (*Cu* 0.84%, *Zn* 79.88%) the primary separation is (α), which is enveloped by (β) as shown in Fig. 2. This enveloping of (β) on (α) indicates that the cooling was fairly rapid and the reaction liquid$+(\alpha)\rightarrow(\beta)$ was not completed, hence we see that the transition point on the liquidus must lie somewhere between the compositions of these alloys *CZA* 3 and 4.

The chill cast alloys *CZA* 5 (*Cu* 1.00%, *Zn* 74.48%) and *CZA* 6 (*Cu* 1.29%, *Zn* 71.40%) show similar structures as in Fig. 2, but they are

changed into the uniform (β), if they are cooled slowly. Fig. 4 shows such a microstructure of the alloy *CZA* 6 quenched at 409° C. after heating for 1 hour at that temperature.

The alloy *CZA* 8 (*Cu* 2.08%, *Zn* 52.97%) consists of (α)+(β)+*CuAl* at 350° C. This is seen in Fig. 5, which shows the needle-like grey crystal *CuAl* in the matrix of white (α) and dark (β), under a magnification of 150 diameters.

Fig. 3 represents the alloy *CZA* 12 containing *Cu* 3.76% and *Zn* 10.93%. In the figure the primary separation (α) appears in dendritic form, surrounded by the eutectic (α)+$CuAl_2$, while in the same alloy quenched at 350° C. after heating for 1 hour $CuAl_2$ is uniformly distributed on the whole ground of (α), as shown in Fig 6.

The chill cast alloy *CZC* 4 (*Cu* 2.62%, *Zn* 85.88%) shows a similar microstructure to *CZA* 3, but the primarily separated (β) is surrounded by the ternary mixtures of (β)+(γ)+(ε) instead of (β)+(γ), as shown in Fig. 7. This ternary mixture is distinguished by the presence of white crystals (ε), which can be more distinctly observed in the microstructure of the chill cast alloy *CZC* 8 (*Cu* 7.87%, *Zn* 61.00%) under a magnification of 320 diameters. (Fig. 8)

Fig. 9 is the microphotograph of the chill cast alloy *CZC* 13 (*Cu* 15.59%, *Zn* 22.50%), in which primary (α) crystals are present in the matrix of the binary mixture (α)+$CuAl_2$, but the (α) is not enveloped by (β) as in Fig. 8.

In the alloy *CZD* 1 (*Cu* 1.49%, *Zn* 95.54%) the (γ) crystals separate primarily, and this alloy solidifies with the reaction liquid→(β)+(γ). This is illustrated in the microphotograph of the chill cast alloy (Fig. 10). When this alloy is for 1 hour annealed at 350° C. and quenched in water, the (β) crystals are distributed in the ground of (γ), as shown under a magnification of 300 diameters in Fig. 11.

Fig. 12 illustrates the microstructure of the chill cast alloy *CZD* 3 (*Cu* 4.51%, *Zn* 84.52%), in which the primary crystallization is (β). In the same alloy annealed and quenched at 350° C. the white crystals of (ε) are distinctly observed in the ground of (β)+(γ). This is shown in Fig.

13, under a magnification of 300 diameters.

But in the alloy *CZD* 5 (*Cu* 7.38%, *Zn* 74.75%), the primary separation is the (α) crystals, which are transformed into (β) with the binary peritectic reaction

$$\text{liquid} + (\alpha) \rightarrow (\beta).$$

Cooling showly, it solidifies with the reaction

$$\text{liquid} + CuAl \rightarrow (\varepsilon) + (\beta) \text{ at } 400^\circ \text{ C.},$$

hence this alloy consists of $(\beta)+(\varepsilon)+CuAl$ at temperatures higher than 300° C. This is shown in Fig. 14. The white (ε) and the light grey crystals *CuAl* are present in the matrix of (β).

However, the alloy *CZD* 8 (*Cu* 11.95%, *Zn* 60.51%) consists of (α) $+(\beta)+CuAl$ at these temperatures, as shown in Fig. 15. Figs. 16 and 17 show the microphotographs of the cast alloys *CZD* 9 and 12. In the former the enveloping of (β) on (α) is evident, and it indicates that the reaction

$$\text{liquid} + (\alpha) \rightarrow (\beta)$$

did not completely take place, but in the latter the primary crystals (α) are only surrounded by the binary eutectic $(\alpha)+CuAl_2$. When this alloy *CZD* 12 is annealed for 1 hour at 400° C. and quenched at the temperature, the crystals of $CuAl_2$ are uniformly distributed in the matrix (α), as in Fig. 18.

Fig. 19 shows the microstructure of the chill cast alloy *CZF* 4 (*Cu* 8.94%, *Zn* 80.25%), in which the binary mixture of $CuAl+(\varepsilon)$ separates primarily, and the reaction liquid $+CuAl \rightarrow (\beta)+(\varepsilon)$ takes place subsequently. Finally, it solidifies with the reaction

$$\text{liquid} + (\varepsilon) \rightarrow (\beta) + (\gamma).$$

Hence such an alloy consists of $(\varepsilon)+(\beta)+(\gamma)$ at the temperature just below the solidus. For example, Fig. 20 shows the microstructure of the similar alloy *CZF* 3, which was annealed at 350° C. and quenched at that temperature. In the figure we see that white crystals (ε) are present with the dark (β) and the light grey (γ) crystals.

CZF 7 is an alloy containing 17.88% of copper and 62.75% of zinc. It commences to solidify with the primary crustallization of *CuAl*, and it

completes it with the reaction liquid + $CuAl \rightarrow (\varepsilon) + (\beta)$, as shown in Fig. 21.

Fig. 22 illustrates the alloy *CZF* 6 (*Cu* 16.01%, *Zn* 65.75%) annealed at 350° C. and quenched, in which we see the light grey crystals *CuAl* being transformed into the white (ε) in the ground of (β), even if this is not so distinct in the photograph.

In the alloy *CZF* 8 (*Cu* 19.37%, *Zn* 52.55%) a similar reaction takes place, but it solidifies into $(\beta) + CuAl$, if it be cooled slowly, hence it consists of $(\beta) + CuAl$ at the temperature 350° C. This is illustrated in Fig. 23, under a magnification of 300 diameters.

We see in the alloys *CZF* 9 (*Cu* 27.10%, *Zn* 42.38%) and *CZF* 10 (*Cu* 30.83%, *Zn* 31.50%) that *CuAl* separates primarily, and it changes into $CuAl_2$, but this reaction seems to proceed without difficulty, as the $CuAl_2$ is present in the chill-cast alloy, as if it were a primary separation.

It is also evident in the diagram that these alloys consist of $(\alpha) + (\beta) + CuAl_2$ at the temperature 350° C. We see such a microstructure in Fig. 24, in which the white crystals of $CuAl_2$ are being transformed into the light grey *CuAl*, and they are distributed in the matrix of the (α) and the decomposed (β).

As seen in this figure, the reaction $CuAl_2 \rightarrow CuAl$ seems not to be completed with such a heat-treatment, as it was annealed for 1 hour at 350° C. and quenched in water.

The similar phenomenon is also observed in the alloy *CZF* 12 (*Cu* 39.42%, *Zn* 12.13%), which was annealed at 350° C. and quenched at that temperature. It is shown in Fig. 25.

Fig. 26 shows the chill cast alloy *CZF* 11 (*Cu* 35.32%, *Zn* 22.31%), in which the primary separation $CuAl_2$ is present in the ternary mixture of $(\alpha) + CuAl + CuAl_2$.

Fig. 27 to 32 illustrate the microstructures of the chill cast alloys of the *CZG* Series. In these alloys we see no peculiar structures to speak of, but we notice in the alloy *CZG* 13 (*Cu* 44.25%, *Zn* 11.23%), that the primary crystals *CuAl* are enveloped by the secondary crystals $CuAl_2$ in angular form.

Fig. 33, under a magnification of 750 diameters, shows the micro-

structure of the alloy *ZF* 7 (*Cu* 9.60%, *Zn* 28.52%) which was heated for 30 minutes at 305° C. and quenched in water.

In this figure we see that the light grey crystal $CuAl_2$ separated during the solidification is changing into the dark grey crystal *CuAl*. In the same alloy heated for 2 hours at 305° C. and quenched, however, we see that the $CuAl_2$ has completely transformed into *CuAl*. Fig. 34 illustrates such a structure, in which the black portion is the decomposed (β).

The alloy *ZF* 3 (*Cu* 10.09%, *Zn* 14.46%) consists of (α)+$CuAl_2$, when it has just solidified, but the $CuAl_2$ is changed into *CuAl* on cooling from about 350° C. Fig. 35 shows such a structure in which some portion of $CuAl_2$ has transformed into *CuAl*.

Fig. 36 is the photo-micrograph of *ZF* 2 (*Cu* 9.90%, *Zn* 8.48%), in which the dark etching constituents are $CuAl_2$ in the matrix of (α). $CuAl_2$ is coloured dark-red, when it is etched with hot concentrated nitric acid.

Many other specimens were also annealed at various temperatures for 1 or 2 hours, and were quenched at the temperature of annealing. Their microstructures were observed, and the results are summarized in the following Table.

Table 26.

The Results of Heat Treatment.

No.	Temperature of Quenching. °C.	Observation.	No.	Temperature of Quenching. °C.	Observation.
		CZA Series.			
CZA 1	352	(β)+(γ)	CZA 6	354	(α)+(β)+CuAl
„ 3	348	(β)+(γ)	„ 6	384	(α)+(β)
„ 4	352	(β)+(γ)	„ 6	392	(β)
„ 4	376	(β)+(γ)	„ 7	357	(α)+(β)+CuAl
„ 4	393	liquid+(β)+(γ)	„ 8	348	(α)+(β)+CuAl
„ 5	352	(β)	„ 9	357	(α)+(β)+CuAl
„ 5	394	(β)	„ 10	348	(α)+CuAl+(β)
„ 5	400	(β)	„ 10	408	(α)+CuAl+$CuAl_2$
„ 5	412	liquid+(β)	„ 11	408	(α)+CuAl+$CuAl_2$

No.	Temperature of Quenching. °C.	Observation.	No.	Temperature of Quenching. °C.	Observation.
		CZB Series.			
CZB 4	350	(β)+(γ)+(ε)	CZB 9	400	(α)+(β)+CuAl
„ 5	350	(β)+(γ)+(ε)	„ 11	400	(α)+(β)+CuAl
„ 6	348	(β)+(ε)	„ 14	350	(α)+(β)+CuAl
„ 7	348	(α)+(β)+CuAl	„ 14	420	(α)+$CuAl_2$
„ 8	426	(α)+(β)+CuAl	„ 15	345	(α)+$CuAl_2$
„ 9	340	(α)+(β)+CuAl	„ 15	380	(α)+$CuAl_2$
		CZC Series.			
CZC 1	325	(β)+(γ)	CZC 9	445	liquid+(α)+CuAl
„ 2	358	(β)+(γ)	„ 11	450	(α)+CuAl+$CuAl_2$
„ 3	358	(β)+(γ)+(ε)	„ 11	438	(α)+CuAl+$CuAl_2$
„ 4	358	(β)+(γ)+(ε)	„ 11	350	(α)+(β)+$CuAl_2$
„ 5	365	(β)+(γ)+(ε)	„ 12	448	(α)+CuAl+$CuAl_2$
„ 6	365	(β)+(γ)+(ε)	„ 12	350	(α)+(β)+$CuAl_2$
„ 7	358	(β)+(ε)+CuAl	„ 13	450	(α)+$CuAl_2$
„ 8	358	(α)+(β)+CuAl	„ 13	350	(α)+CuAl+$CuAl_2$
„ 9	370	(α)+(β)+CuAl	„ 14	370	(α)+$CuAl_2$
„ 9	410	(α)+(β)+CuAl	„ 14	350	(α)+$CuAl_2$
		CZD Series.			
CZD 1	355	(β)+(γ)	CZD 7	355	(β)+(ε)+CuAl
„ 3	355	(β)+(γ)+(ε)	„ 9	360	(α)+(β)+CuAl
„ 4	370	(β)+(γ)+(ε)	„ 10	370	(α)+(β)+CuAl
„ 5	330	(β)+(ε)+CuAl	„ 11	410	(α)+(β)+CuAl
„ 6	370	(β)+(ε)+CuAl	„ 12	400	(α)+$CuAl_2$
„ 6	400	(β)+(ε)+CuAl	„ 13	355	(α)+$CuAl_2$
		CZE Series.			
CZE 1	350	(β)+(γ)	CZE 6	350	(β)+(ε)+CuAl
„ 2	360	(β)+(γ)+(ε)	„ 7	360	(α)+(β)+CuAl
„ 3	350	(β)+(γ)+(ε)	„ 9	360	(α)+(β)+CuAl
„ 4	350	(β)+(γ)+(ε)	„ 10	360	(α)+(β)+CuAl
„ 5	350	(β)+(ε)+CuAl	„ 11	360	(α)+(β)+CuAl
			„ 12	360	(α)+$CuAl_2$

No.	Temperature of Quenching. °C.	Observation.	No.	Temperature of Quenching. °C.	Observation.
		CZF Series.			
CZF 1	370	(β)+(γ)	CZF 8	370	(β)+CuAl
„ 2	350	(β)+(γ)+(ε)	„ 9	350	(α)+(β)+CuAl
„ 4	350	(β)+(γ)+(ε)	„ 10	350	(α)+(β)+CuAl
„ 5	370	(β)+(ε)+CuAl	„ 11	350	(α)+(β)+CuAl
„ 6	370	(β)+(ε)+CuAl	„ 12	350	(α)+CuAl+$CuAl_2$
		CZG Series.			
CZG 1	350	(β)+(γ)	CZG 8	350	(β)+(ε)+CuAl
„ 3	350	(β)+(γ)+(ε)	„ 9	350	(β)+(ε)+CuAl
„ 4	350	(β)+(ε)	„ 11	350	(α)+(β)+CuAl
„ 5	350	(β)+(ε)+CuAl	„ 12	350	(α)+(β)+CuAl
„ 6	350	(β)+(ε)+CuAl	„ 13	350	(α)+(β)+CuAl

PHENOMENA OF SOLIDIFICATION AND SOLID TRANSFORMATION.

Summing up the results of our present investigation, we want now to describe the phenomena of solidification and the solid transformation in the state of equilibrium, referring to the general equilibrium diagram (Fig. 32)

a) Phenomena of Solidification.

Now the alloy in the region Eiss' separates primarily the solid solution (α). With cooling the mother liquor varies its composition and when it reaches the line *EO*, the univariant reaction liquid$\rightarrow(\alpha)+CuAl_2$ begins. With cooling, the mother liquor and the (α) vary their compositions along *EO* and *is* respectively. But we assume that $CuAl_2$ has no solubility in ternary alloys. As the mother liquor disappears in this reaction, the alloy completes its solidification.

Similarly the alloy in *sOs'* deposits (α), and then (α) and $CuAl_2$

together. But the mother liquor still remains, even if its composition reaches the point O, where the reaction.

$$\text{liquid} + CuAl_2 \rightarrow (\alpha)_s + CuAl$$

takes place at a constant temperature 450° C. and, according as the composition of the alloy exists in $ss't'$ or $t'sO$, the solidification finishes at this invariant point or the mother liquor remains. From the remaining liquid $CuAl$ and (α) deposit simultaneously, and the solidification ends in this univariant reaction or in the reaction at the point P.

If the alloy has its composition in $Khs'O$, $CuAl$ or $CuAl_2$ primarily separates, and after the reaction on CS, DO, or EO occurs, the residual melts reach the point O and the reaction

$$\text{liquid} + CuAl_2 \rightarrow (\alpha)_s + CuAl$$

takes place in the same way.

In short, the invariant reaction at O is observed in the region $KhsO$, and the alloys in Khs end their solidification at the temperature of this reaction, but in KsO the liquid still remains, even if this reaction is completed.

In the region $OstP$, the reaction liquid$\rightarrow(\alpha)+CuAl$ occurs after the primary separation of (α), and in this reaction (α) varies its composition along st. When the residual melts come to the point P, the reaction

$$\text{liquid} + (\alpha)_t \rightarrow (\beta)_l + CuAl$$

takes place, and the alloy in $u't'l'm'$ completes its solidification at this temperature, but in $Om'l'P$ it changes into the reaction liquid$\rightarrow CuAl+(\beta)$ with cooling.

Similarly, (α) separates primarily in the region Ptl and then occurs the peritectic reaction

$$\text{liquid} + (\alpha) \rightarrow (\beta),$$

at which (α) changes along at, and (β) along bl. Solidification ends at the invariant reaction at P or liquid still remains, according as the composition of the alloy exists in $ll't$ or $Pl'l$.

But in *PlbF* the reaction liquid$+(\alpha)\rightarrow(\beta)$ finishes, before the melts reach the point *P*, and they change into the reaction liquid$\rightarrow(\beta)$.

Notwithstanding the manner in which the primary and secondary separations may occur, the reaction at *P* takes place in the region represented by *KlP*, and the alloys in *Kl* solidify at the temperature of *P*, while in *KlP* the mother liquor remains and changes into the reaction on *PQ*.

The region of the primary separation of (β) is represented by *FGR QP*. In this region, the reaction of secondary separation differs according to the original composition of the alloy, i. e, the reaction on *PQ*, *QR* or *GR* occurring secondarily.

If the melts have come to the point on *PQ*, the binary eutectic reaction

$$\text{liquid}\rightarrow(\beta)+CuAl$$

begins to occur, and as the reaction proceeds, the (β) varies its composition along *lm*. Finally it changes into the reaction

$$\text{liquid}+CuAl\rightarrow(\beta)_m+(\varepsilon)_{k_1}.$$

On the other hand, the alloy in *n'k'RQ* separates (β) and (ε) altogether, after the (β) is separated primarily, and then it changes into the peritecto-eutectic reaction

$$\text{liquid}+(\varepsilon)_k\rightarrow(\beta)_n+(\gamma)_o.$$

While in the region *FGRk'* the residual melt comes to the point on *RG* after the primary separation of (β), and it deposits (β) and (γ) at the same time with the eutectic reaction liquid$\rightarrow(\beta)+(\gamma)$, at which (β) and (γ) change respectively along *nc* and *od*.

The primary separation of (γ) takes place in the region *GBHR*, and the secondary crystallization is represented by the reaction

$$\text{liquid}\rightarrow(\beta)+(\gamma)$$

in this region.

HISQR represents the region of the primary separation of (ε). The alloys in this region separate (ε) primarily, and then the reaction on *SQ*, *QR*, or *HR* takes place according to the original composition of the

alloy. Accordingly the solidification is completed at the point Q or R, or sometimes with the reaction on RH.

$CuAl$ is primarily crystallized in $CDOPQS$, and in the alloys of this region the mother liquor comes to the point on DO, OP, PQ, or SQ with cooling, at which begin the reactions,

$$\text{liquid} + CuAl \rightarrow CuAl_2,$$
$$\text{liquid} \rightarrow CuAl + (\alpha),$$
$$\text{liquid} \rightarrow CuAl + (\beta),$$
or
$$\text{liquid} \rightarrow CuAl + (\varepsilon).$$

The solidification is completed with one of these binary reactions, or with the invariant reaction at O, P, or Q.

As already mentioned, the invariant points Q and R represent the peritecto-eutectic reaction, which takes place in the region $KmQk_1$ and $nRok$ respectively.

So far we have explained the phenomena of solidification in the important part of the diagram. Finally, in Table 25, the liquidus, the planes of binary separation, the solidus surfaces, and the planes of invariant reactions are summarized.

Table 27.

Reaction Surfaces on Solidification.

Primary Separation.	Reaction.	Region.	Points or lines, through which the reaction generator passes.
(α)	Liquid $\rightleftarrows$ (α)	EAFPO	——
	Liquid $\rightleftarrows$ (α)+$CuAl_2$	EisO	EO-is
	Liquid $\rightleftarrows$ (α)+CuAl	OstP	OP-st
	Liquid +(α) $\rightleftarrows$ (β)	aFPt	FP-at
	Liquid $\rightleftarrows$ (β)	bFPl	FP-bl
	(α)	Aatsi	——
	(β)	bcnml	——
	(α)+(β)	ablt	at-bl

Primary separation.	Reaction.	Region.	Points or lines, through which the reaction generator passes.
(β)	Liquid $\rightleftarrows$ (β)	FGRQP	——
	Liquid $\rightleftarrows$ CuAl+(β)	PlmQ	PQ-lm
	Liquid $\rightleftarrows$ (β)+(ε)	mnRQ	RQ-mn
	Liquid $\rightleftarrows$ (β)+(γ)	ncGR	RG-nc
(γ)	Liquid $\rightleftarrows$ (γ)	GBHR	——
	Liquid $\rightleftarrows$ (β)+(γ)	GdoR	RG-od
	(γ)	Beod	——
	(β)+(α)	cdon	nc-od
(ε)	Liquid $\rightleftarrows$ (ε)	HISQR	——
	Liquid $\rightleftarrows$ (ε)+(γ)	RHfk	RH-kf
	Liquid $\rightleftarrows$ (β)+(ε)	QRkk$_1$	QR-kk$_1$
	Liquid $\rightleftarrows$ (ε)+CuAl	SQkg$_1$	SQ-kg$_1$
	Liquid $\rightleftarrows$ (γ)	RHeo	HR-eo
	(ε)	fkk$_1$g$_1$g	——
	(γ)+(ε)	oefk	oe-kf
	(β)+(ε)	nkk$_1$m	mn-kk$_1$
CuAl	Liquid $\rightleftarrows$ CuAl	CDOPQS	——
	Liquid + CuAl $\rightleftarrows$ CuAl$_2$	KDO	DO-KK
	Liquid $\rightleftarrows$ (α)+CuAl	KOP	OP-KK
	Liquid $\rightleftarrows$ (β)+CuAl	KPQ	PQ-KK
	Liquid $\rightleftarrows$ (ε)+CuAl	KQS	SQ-KK
	Liquid $\rightleftarrows$ CuAl$_2$	DOh	DO-hh
	(α)+CuAl	Kst	st-KK
	( )+CuAl	Klm	lm-KK
CuAl$_2$	Liquid $\rightleftarrows$ CuAl$_2$	DEO	——
	Liquid $\rightleftarrows$ (α)+CuAl$_2$	hEO	EO-hh
	(α)+CuAl$_2$	his	is-hh

Primary Separation.	Reaction.	Region.	Points or lines, through which the reaction generator passes.
Invariant point.	Liquid + $CuAl_2 \rightleftarrows (\alpha)+CuAl$	KhsO	O
	Liquid + $(\alpha) \rightleftarrows (\beta)+CuAl$	KtlP	P
	Liquid + $CuAl \rightleftarrows (\beta)+(\varepsilon)$	mQk_1K	Q
	Liquid + $(\varepsilon) \rightleftarrows (\beta)+(\gamma)$	nRok	R
	Liquid + $(\delta) \rightleftarrows (\varepsilon)+CuAl$	KSg_1	S

In this table, the reaction planes, which exist over the region of the primary crystallization of 2 kinds, are given on one side of them, and we denote, for example, by the reaction liquid→(β) in the region of the (α), that the reaction commences on this plane after the reaction liquid + (α)→ (β) ends.

b) Solid Transformation.

When solidification has just completed, it is apparent from the diagram that the alloys consist of the phases as given in the following Table, according to their composition. Here we assume that *CuAl*, $CuAl_2$ have no solubility in ternary alloys.

Table 28.

Field.	Existing Phases.	Field.	Existing Phases.
iAats	(α)	lmK	(β)+CuAl
bcnml	(β)	stK	(α)+CuAl
dBeo	(γ)	ish	(α)+$CuAl_2$
fgg_1k_1k	(ε)	Khs	(α)+$CuAl_2$+CuAl
ablt	(α)+(β)	Ktl	(α)+(β)+CuAl
cdon	(β)+(γ)	Kmk_1	(β)+(ε)+CuAl
efko	(γ)+(ε)	nok	(β)+(γ)+(ε)
k_1mnk	(ε)+(β)		

As shown in Table 28, there exist *CuAl*, $(\beta)_m$ and $(\varepsilon)_{k_1}$ together in the alloys of the region Kmk_1, when they have just solidified. With cooling, the solubility of *CuAl* and (ε) in (β) varies along mx, i. e., the (β) separates *CuAl* and (ε), and its composition changes along mx.

When the composition of (β) has come to x, the solubility of (γ) in (β) reaches also its limit, and the invariant reaction

$$(\beta)_x + (\varepsilon)_{f_1} \rightarrow CuAl + (\gamma)_j$$

takes place.

On the other hand, the alloys in the field *nok* consist of $(\beta)_n$, $(\gamma)_o$ and $(\varepsilon)_k$, when solidification is completed. Similarly, this (β) changes its composition along nx with cooling, separating (ε) and (γ), while the (γ) varies along oj at the same time, separating (β) and (ε). Also (ε) changes its composition along kf_1. When the (β), (γ), and (ε) have reached the compositions represented by x, j, and f_1 respectively, the solubility of *CuAl* in them arrives here at the limit of saturation, and the reaction

$$(\beta)_x + (\varepsilon)_{f_1} \rightarrow CuAl + (\gamma)_j$$

commences.

In short, this invariant reaction takes place in the region $Kxjf_1$, and at this reaction the (β) disappears in the alloys of Kjf_1, but in the alloys of Kxj the (ε) disappears, and (β), (γ), and *CuAl* remains.

In the latter case, the (β) and (γ) still change their compositions along xy and jw with cooling. The solubility of (α) in (β) reaches its saturation at y, and the invariant reaction

$$(\beta)_y + CuAl \rightarrow (\alpha)_v + (\gamma)_w$$

begins.

In the field *Ktl* the alloys consist of $(\alpha)_t$, $(\beta)_l$ and *CuAl* immediately after solidification. With cooling, this (α) and (β) change their compositions along tv, and ly respectively.

When the (α) and (β) have arrived at v and y, they become saturated with (γ), and similarly the invariant reaction

$$(\beta)_y + CuAl \rightarrow (\alpha)_v + (\gamma)_w$$

commences.

After all in the field *Kvyw* the above invariant reaction takes place, at which (β) dissociates completely into (α) and (γ) in the alloys of *Kvw*, while in the alloys *vyw* *CuAl* disappears at this reaction, and $(\alpha)_v$, $(\beta)_y$, and $(\gamma)_w$ remain.

In the latter case, these (α), (β), and (γ) change their compositions along *vp*, *yq*, and *wr* respectively; in other words, the (β) continues to dissociate into (α) and (γ) along *yq*, and this dissociation completes on some points of *yq*.

From the above explanation we see that there exists a region where either of the 2 invariant reactions take place in the same alloy, and in the other field one of them is observed, as was already proved by our experiments.

When the alloys in the field *Kst* have just crystallized, they consist of (α)$_s$, *CuAl* and $CuAl_2$, but with cooling the (α) varies along *su*, separating *CuAl* and $CuAl_2$ altogether.

Finally, in Table 29, we summarize the reaction planes in the solid state.

Table 29.

Reaction Planes in Solid State.

Reaction.	Field.	Points or lines, through which the reaction generator passes.	Remarks.
$(\alpha) \rightleftarrows (\beta)$	atvp	—	—
$(\alpha) \rightleftarrows (\gamma)$	zp′pv	—	—
$(\alpha) \rightleftarrows$ CuAl	suzt	—	—
$(\alpha) \rightleftarrows CuAl_2$	ii′us	—	—
$(\beta) \rightleftarrows (\alpha)$	bqyl	—	—
$(\beta) \rightleftarrows (\gamma)$	cnxyq	—	—
$(\beta) \rightleftarrows (\varepsilon)$	mxn	—	—
$(\beta) \rightleftarrows$ CuAl	lyxm	—	—
$(\gamma) \rightleftarrows (\alpha)$	rr′w′w	—	—
$(\gamma) \rightleftarrows (\beta)$	drwjo	—	—

Reaction.	Field.	Points or lines, through which the reaction generator passes.	Remarks.
$(\gamma) \rightleftarrows CuAl$	jww′j′	——	——
$(\gamma) \rightleftarrows (\varepsilon)$	eojj′e′	——	——
$(\alpha)+(\beta) \rightleftarrows CuAl$	tvyl	tv-ly	——
$(\alpha)+(\gamma) \rightleftarrows CuAl$	vzw′w	vz-ww′	——
$(\alpha)+CuAl \rightleftarrows (\beta)$	Kvt	tv-KK	——
$(\alpha)+CuAl_2 \rightleftarrows CuAl$	hus	su-hh	The reaction bigins.
$(\alpha)+CuAl_2 \rightleftarrows CuAl$	Ksu	su-KK	The reaction ends.
$(\alpha)+CuAl \rightleftarrows (\gamma)$	Kzv	vz-KK	——
$(\beta)+(\gamma) \rightleftarrows (\varepsilon)$	onxj	nx-oj	——
$(\beta)+(\gamma) \rightleftarrows CuAl$	xywj	xy-jw	——
$(\beta) \rightleftarrows (\alpha)+(\gamma)$	vpqy	vp-yq	The reaction begins.
$(\beta) \rightleftarrows (\alpha)+(\gamma)$	yqrw	yq-wr	,,
$(\beta) \rightleftarrows (\alpha)+(\gamma)$	vprw	vp-rw	The reaction ends.
$(\beta)+(\varepsilon) \rightleftarrows (\gamma)$	kf_1xn	$nx\text{-}kf_1$	——
$(\beta)+(\varepsilon) \rightleftarrows CuAl$	k_1mxf_1	$mx\text{-}k_1f_1$	——
$(\beta)+CuAl \rightleftarrows (\varepsilon)$	Kxm	xm-KK	——
$(\beta)+CuAl \rightleftarrows (\gamma)$	Kyx	xy-KK	——
$(\beta)+CuAl \rightleftarrows (\alpha)$	Kly	ly-KK	——
$(\gamma)+CuAl \rightleftarrows (\varepsilon)$	Koj′	ojj′-KK	——
$(\gamma)+(\varepsilon) \rightleftarrows (\beta)$	kf_1jo	$oj\text{-}kf_1$	——
$(\gamma)+(\varepsilon) \rightleftarrows CuAl$	$f_1jj'f_2$	$jj'\text{-}f_1f_2$	——
$(\varepsilon)+CuAl \rightleftarrows (\beta)$	Kk_1f_1	$k_1f_1\text{-}KK$	——
$(\varepsilon)+CuAl \rightleftarrows (\gamma)$	Kf_1f_2	$f_1f_2\text{-}KK$	——
$(\beta)+(\varepsilon) \rightleftarrows CuAl+(\gamma)$	$Kxjf_1$	x	——
$(\beta)+CuAl \rightleftarrows (\alpha)+(\gamma)$	Kvyw	y	——

According to Hanson and Gayler, the invariant point of such reaction as

$$(\beta)+(\varepsilon) \rightleftarrows CuAl+(\gamma)$$

in the solid state is represented by the intersecting point on the line Kj and f_1x, but it is evident from the above explanation that such a point does not illustrate the invariant point, showing the above reaction, and it gives the point, where the reaction takes place in a maximum amount. In the solidification we adopt such a point O on the liquidus surface as the invariant point of the reaction

$$\text{liquid} + CuAl_2 \rightarrow CuAl + (\alpha).$$

Similarly, we must take x as the ternary transition point of the (β).

SUMMARY.

(1) The constitution of the alloys of aluminium, copper, and zinc was investigated, and the equilibrium diagram on the side of aluminium and zinc was determined.

(2) The differential thermal analyses were not only employed for the study of the phenomena of solidification, but also to determine the solid transformation.

(3) The peritecto-eutectic reactions

$$\text{liquid} + (\alpha) \rightleftarrows (\beta) + CuAl,$$
$$\text{liquid} + CuAl \rightleftarrows (\beta) + (\varepsilon),$$
$$\text{liquid} + (\varepsilon) \rightleftarrows (\beta) + (\gamma),$$

and

$$\text{liquid} + (\delta) \rightleftarrows CuAl + (\varepsilon)$$

were all determined to exist, as given by Jareš, Hanson and Gayler, but the reaction

$$\text{liquid} + CuAl_2 \rightleftarrows CuAl + (\beta)$$

was not observed, and a new peritecto-eutectic reaction

$$\text{liquid} + CuAl_2 \rightleftarrows (\alpha) + CuAl$$

was found.

(4) The (β) solution was found experimentally to transform in 2 steps with the reactions

$$(\beta) + (\varepsilon) \rightleftarrows CuAl + (\gamma)$$

and

$$(\beta) + CuAl \rightleftarrows (\alpha) + (\gamma)$$

in the ternary system.

PART II.
THE AGE-HARDENING OF ALUMINIUM-RICH ALLOYS OF ALLUMINIUM, COPPER, AND ZINC.

INTRODUCTION.

The present writer has published an investigation on the age-hardening properties of aluminium-rich alloys of aluminium and zinc[1]. In relation to that investigation, the present work has been made to study the influence of copper upon the ageing properties of aluminium-rich alloys of aluminium and zinc.

As well known, aluminium alloys containing copper and zinc are used widely in industry, e. g., in the machine parts of aero-engines or automobile engines. Among them a cast alloy known as *L* 5 (*Cu* 2.5–3.0%, *Zn* 12.5–14.5%) is the most important.

It has been already known that this alloy shows age-hardening even in casting, and its mechanical properties can be improved by heat-treatment[1]. But there has been no systematic investigation on the age-hardening of *Al*-rich *Al-Cu-Zn* alloys. Our present research has been, therefore, undertaken to investigate systematically the effect of heat-treatment on the properties of the alloy in the first place. Then an investigation on the ageing phenomena of *Al*-rich *Al-Cu-Zn* alloys has been carried out. Finally the present writer has tried to explain the mechanism of hardening due to ageing.

HEAT TREATMENT OF *L* 5 ALLOY.

The specimens employed in the present experiment had the compositions as given in the following table.

Table 1.

No.	Composition (by analysis).		
	Cu %	Zn %	Al %
LA	1.09	13.73	remainder
LB	3.22	13.92	,,

(1) Memoirs of the College of Engineering, Kyoto Imp. Univ., 3 (1924), 133.
(2) Vickers, Metals and Their Alloys, 249.

a) Effect of quenching temperature on ageing.

These specimens were heated for 30 minutes at 500°, 450°, 400°, and 320° C. respectively in an electric furnace and quenched in water at 30° C. On being quenched, Brinell hardness was immediately measured of the specimens, and then they were aged in a thermostat kept at 30° C. Hardness was also measured in 1 hour after, 2 hours after, and so on.

The results of experiments are summarized in Table 2.

Table 2.

Brinell Hardness of Quenched Alloys.

Temperature of Quenching.	No.	Brinell Hardness. (500 kg. Pressure, 10 mm. Ball, 30 sec.)										
		Immediately after.	1 hr. after.	2 hrs. after.	3 hrs. after.	4 hrs. after.	5 hrs. after.	20 hrs. after.	30 hrs. after.	50 hrs. after.	70 hrs. after.	100 hrs. after.
500°C.	LA	55.0	68.5	72.0	70.2	69.4	65.0	68.8	68.8	68.8	70.0	69.4
	LB	70.0	81.2	77.0	82.4	82.4	84.8	86.0	86.0	86.6	86.6	86.6
450°C.	LA	54.0	58.4	59.8	62.8	59.0	63.0	64.2	65.8	65.8	65.0	65.8
	LB	74.0	83.6	86.0	83.0	80.0	80.0	77.6	80.0	80.0	83.0	80.0
400°C.	LA	52.0	61.0	63.0	64.0	63.0	61.0	61.0	61.0	61.0	61.0	61.0
	LB	74.0	75.2	72.0	70.4	70.0	70.4	70.4	70.4	73.6	70.8	70.8
320°C.	LA	51.0	56.0	58.0	59.0	57.0	59.0	59.0	59.0	61.0	59.5	61.0
	LB	70.0	70.0	70.0	70.0	70.0	70.0	70.0	70.0	70.0	70.0	70.0

As seen from these results, age-hardening was observed to occur in either of the alloys and it was marked in the alloy quenched at the higher temperature. Also we see that the alloy containing 3 per cent. of copper was harder than that of less content of copper, but on the contrary the effect of ageing was marked in the latter alloy.

It is interesting to notice in either of the alloys that hardening took place rapidly at the begining of ageing, then a slight softening was followed, and finally gradual hardening occured. This phenomenon was observed distinctly in the alloy quenched at the higher temperature, but

it was hardly recognised in the alloy quenched at the lower temperature.

The phenomena that hardening took place in 2 steps can be easily explained from the constitution of these alloys. Referring to the equilibrium sections given in Part 1, we see that an alloy containing about 1 to 3 per cent. of copper and about 13.5 per cent. of zinc consists of $(\alpha)+CuAl_2$ at higher temperatures, and, on being slowly cooled to the room temperature, they are changed into $(\alpha)+(\gamma)+CuAl$. In order that $(\alpha)+CuAl_2$ transform into $(\alpha)+(\gamma)+CuAl$, two steps of reactions are necessary to occur; e. i., the transformation of $CuAl_2$ to $CuAl$ and the separation of (γ) and $CuAl$ from (α). Consequently, it might be said that the hardening in two steps was due to these two reactions. But the latter reaction was presumably the chief cause of hardening, because ageing effect was found to be much distinguished in the alloy containing less amount of copper.

b) Effect of tempering upon tensile strength.

Fig. 1,

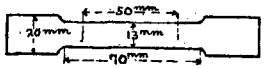

Materials necessary to prepare specimens were melted in a graphite crucible lined with magnesia, which was heated in a gas-fired furnace. At 695°–700° C. they were cast in a chill mould. Test specimens were prepared of these chill cast bars by machining them to the size as given in Fig. 1.

The specimens were annealed at 450° C. for 2 hours, and they were heated again at 450° C. and quenched at that temperature in water (30° C.) Subsequently they were tempered at various temperatures as given in Table 3. After tempering tensile strength was measured.

Tensile testing was made with 7,500 kg. Olsen Tensile Testing Machine, Martens' extensometer being set on the specimen. Thus we obtained the breaking load and the limit of elasticity of the specimen.

The results of experiment are summarized in Table 3, and plotted in Fig. 2.

The figures in the table are an average of two tests, and a load, at which one or two thousandth of mm. of permanent set was just produced,

is given as an elastic limit.

Table 3.

Tensile Properties of Tempered Alloys.

No.		Temperature of Tempering.						
		100°C.	150°C.	200°C.	250°C.	300°C.	350°C.	Aged for 200 hrs.
LA	Tensile Strength (kg./mm^2.).	21.4	21.9	20.7	23.3	23.9	23.8	24.0
	Elastic Limit (kg./mm^2.).	4.6	5.0	7.5	4.9	5.0	4.4	4.7
	Elongation in 5cm. %.	2.9	2.9	2.9	2.5	2.3	3.0	2.7
	Reduction of Area. %.	8.1	7.9	8.1	7.1	7.3	7.9	8.1
LB	Tensile Strength (kg./mm^2.).	24.1	24.0	21.4	23.7	20.8	23.7	26.1
	Elastic Limit (kg./mm^2.).	6.7	5.8	5.7	7.6	6.3	6.7	6.7
	Elongation in 5 cm. %.	1.4	6.0	3.2	4.5	3.0	3.8	2.0
	Reduction of Area. %.	4.0	5.8	4.0	4.1	3.7	4.2	3.0

As seen in the table, the strength of these alloys was somewhat improved by tempering at the temperature higher than 250° C., but on the contrary heating at 200° C. resulted in a slight diminution of strength. The highest value of strength was given by an alloy aged at room temperature for 50 hours. Especially it is to be noted that the alloy *L* 5 has a comparatively low limit of elasticity, even though the breaking load is fairly high as cast aluminium alloys.

Fig. 2.

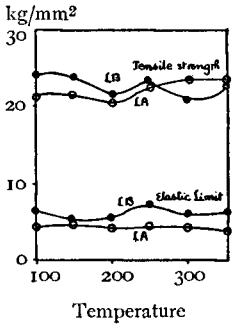

c) Effect of tempering upon hardness.

Specimens were cut off from the same chill cast bars employed for the tensile test, and they were subjected to the similar heat-treatment as was done in tensile test pieces.

In our present experiment Brinell hardness was measured of these

specimens tempered immediately after quenching and tempered after ageing for 50 hours at room temperature respectively.

In Table 4, we summarize the results of measurement.

Table 4.

Brinell Hardness of Tempered Alloys.

	No.	Brinell Hardness. (500 kg. Pressure, 10 mm. Ball, 30 sec.)									
		Immediately after quenching.	50°C.	70°C.	100°C.	150°C.	200°C.	250°C.	300°C.	350°C.	Chill cast.
Tempered immediately after quenching.	LA	46.0	46.0	—	45.0	43.0	45.0	45.0	45.0	43.0	46.0
	LB	56.5	57.0	—	56.5	57.0	60.5	54.0	50.0	58.0	57.0
Tempered 50 hours after quenching.	LA	44.0	—	43.5	44.0	38.5	40.0	44.5	44.5	43.0	46.0
	LB	58.5	—	56.5	56.5	50.0	54.0	61.0	56 0	57.0	57.0

Fig. 3.

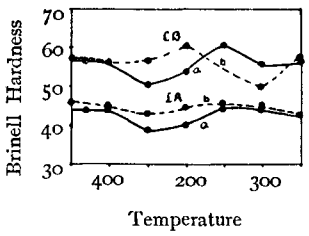

As seen in Fig. 3, the effect of tempering was more distinct than in tensile test. In these alloys the interesting feature is in the fact that tempering at 150° C. resulted in a slight diminution of hardness and a maximum of hardening was found to occur at 200°–250° C. This is a similar phenomenon as was observed in tensile tests.

Also it is worth while to notice that hardening due to tempering at 200°–250° C. was more distinct, contrary to the case of ageing at 30° C., in the alloy containing 3 per cent. of copper. In this case, therefore, the transformation of $CuAl_2$ can be supposed to be the chief cause of hardening at 200°–250° C.

EFFECT OF COMPOSITION UPON HARDENING.

There have been published many investigations upon the phenomena of ageing. However, it can be said that we know nothing of the systematic relation between age-hardening and the composition of alloys. In

our present research, hardness tests were made of series of alloys whose copper content was constant, and whose zinc content varied from zero to 20 per cent., and in this way we have tried to obtain the relationship between hardening and the constitution of alloys.

The chemical analyses of specimens and their Brinell hardness at chill cast state are given in Table 5.

Table 5.

Brinell Hardness of Chill Cast Alloys.

No.	Composition (by analysis).			Brinell Hardness. (500 kg. Pressure, 10 mm. Ball, 30 sec.)
	Cu %	Zn %	Al %	
A 1	0.72	4.76	remainder	26.8
„ 2	0.74	7.72	„	36.3
„ 3	0.75	13.22	„	45.5
„ 4	0.82	16.36	„	54.7
„ 5	0.75	19.75	„	57.5
B 1	1.70	3.97	remainder	34.5
„ 2	1.76	8.69	„	41.0
„ 3	1.63	12.34	„	45.8
„ 4	1 68	16.33	„	65.0
„ 5	1.76	18.47	„	70.5
C 1	3.05	4.29	remainder	39.8
„ 2	3.15	8.01	„	44.3
„ 3	3.15	12.78	„	63.0
„ 4	3.25	15.88	„	71.5
„ 5	3.20	20.57	„	74.0
D 1	4.30	4.49	remainder	41.0
„ 2	4.68	8.52	„	47.5
„ 3	4.58	12.39	„	59.0
„ 4	5.01	16.26	„	70.0
„ 5	4.60	20.00	„	83.0

These chill cast specimens were annealed at 450° C. to remove the heterogeneity of casting. Then they were heated again at 500° C. for 30 minutes and quenched in water at 100°, 75°, 50° and 0° C. respectively.

Immediately, Brinell hardness was measured of them, using 500 kg. pressure and 10 mm. ball. No sooner the hardness was measured, than the specimens were transferred into a thermostat kept at the same temperature as that of the quenching bath. However, the specimen quenched in ice water was aged in ice water contained in a Duwar flask. At these temperatures they were kept for 24 hours and Brinell hardness was measured in 2 hours after and 24 hours after respectively.

Fig. 4.

A Series.

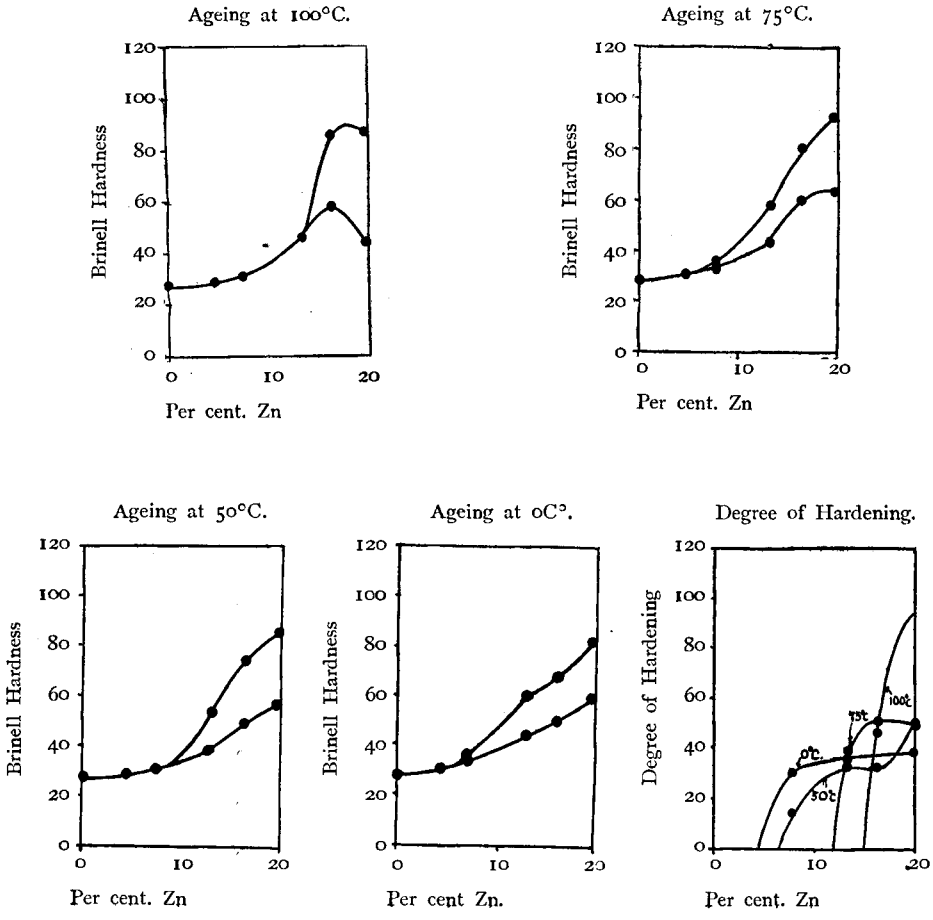

Fig. 5.

B Series.

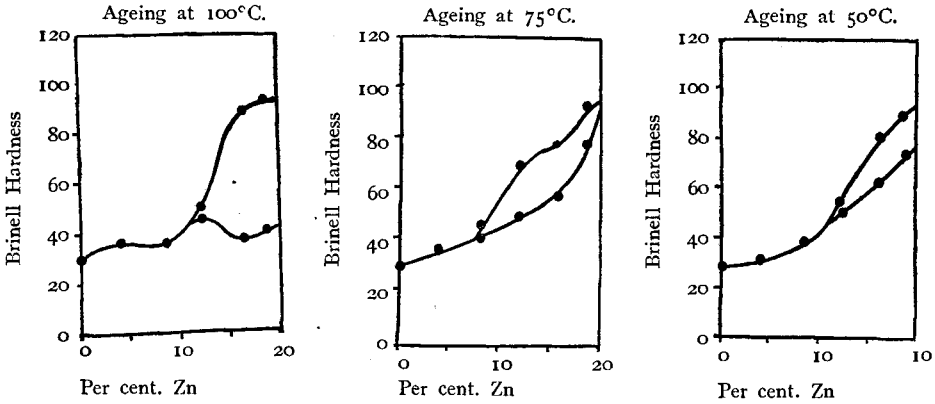

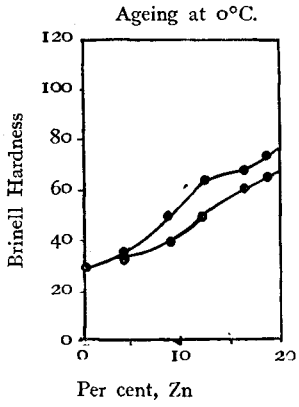

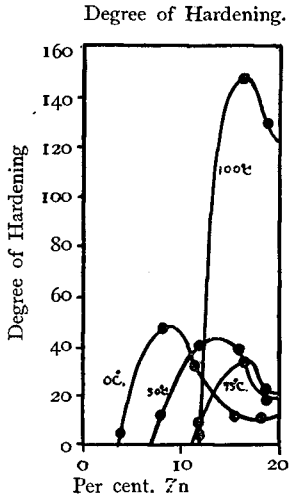

Fig. 6.

C Series.

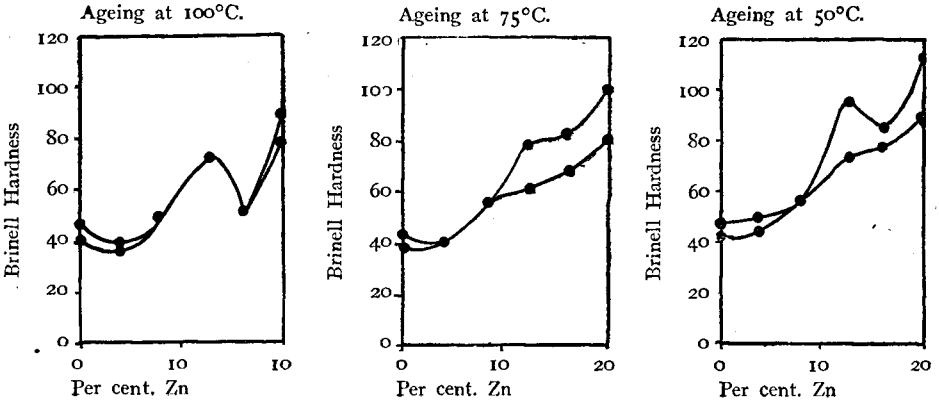

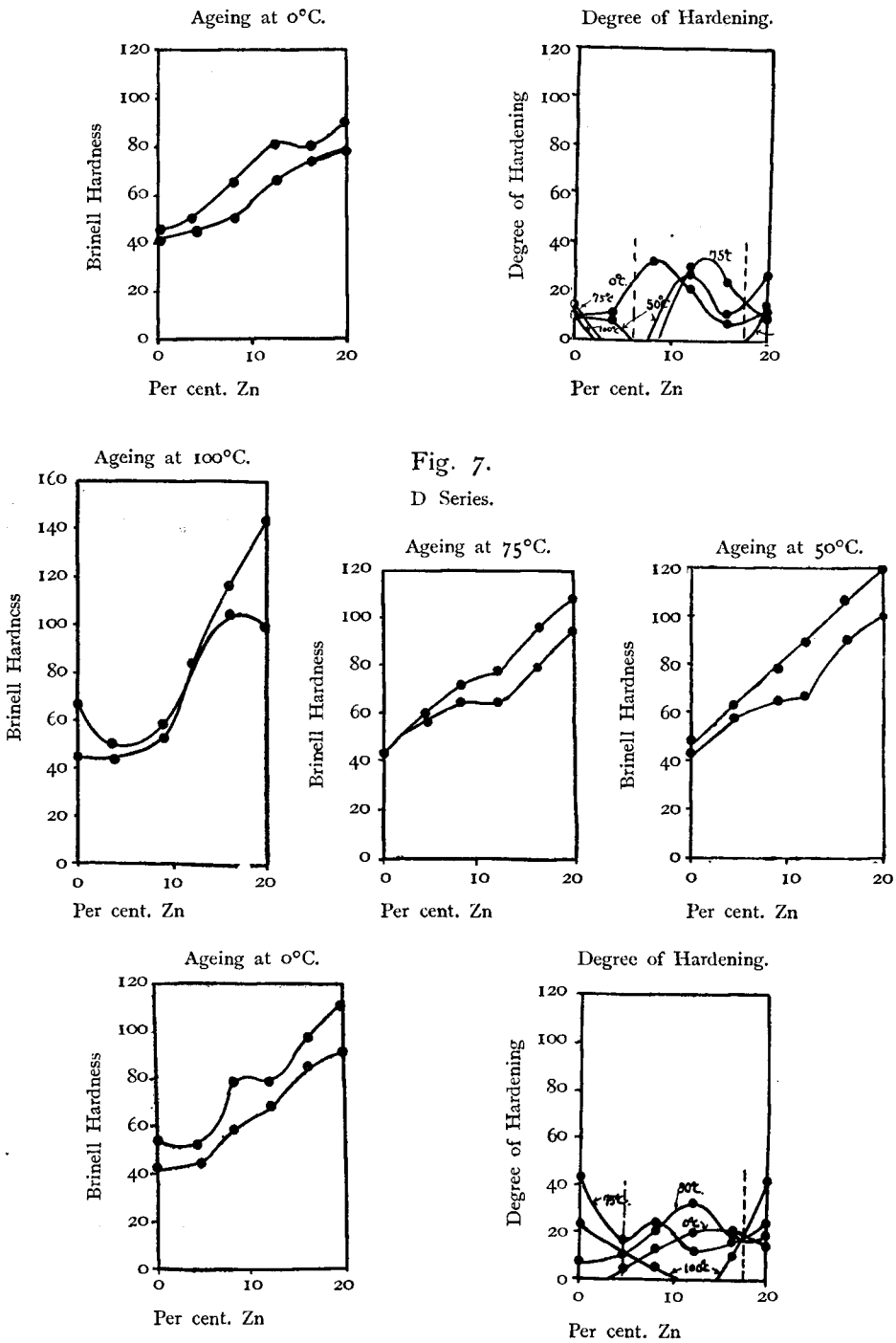

Fig. 7.

D Series.

The results of experiment are summarized in Tables 6 to 9 inclusive, and plotted in Figs. 4 to 7. As seen in these tables, the degree of hardening in different alloys can not be directly compared with the number of hardening, because hardness itself is different in alloys whose compositions are different. As the measure of hardening, therefore, we adopted the percentage increase of hardening in ageing.

Table 6.

Age-hardening at 0° C.

No.	Brinell Hardness. (500 kg. Pressure, 10 mm. Ball, 30 sec.)				
	Immediately after.	2 hours after.	24 hours after.	Hardening in 24 hours.	
				Number.	Degree.
A 1	30.0	30.5	31.8	—	—
„ 2	34.5	43.0	45.5	11.0	31.0
„ 3	44.7	55.0	61.0	16.3	36.5
„ 4	49.0	57.0	68.3	19.3	39.3
„ 5	59.5	61.0	83.0	23.5	39.4
B 1	33.5	38.0	35.5	2.0	5.9
„ 2	37.5	45.0	55.5	18.0	48.0
„ 3	49.0	54.0	65.5	16.0	33.7
„ 4	60.0	71.0	67.5	7.5	12.5
„ 5	65.0	70.0	73.0	8.0	12.3
C 1	45.0	45.0	50.0	5.0	10.9
„ 2	49.5	53.5	66.0	16.5	33.3
„ 3	66.0	78.5	81.0	15.0	22.7
„ 4	72.5	73.0	78.0	5.5	7.6
„ 5	78.0	85.0	89.0	11.0	14.1
D 1	56.0	57.5	59.3	3.3	5.9
„ 2	65.0	68.0	72.5	7.5	11.5
„ 3	64.0	70.0	78.0	14.0	21.9
„ 4	80.0	80.0	97.5	17.5	21.8
„ 5	96.0	109.0	111.0	15.0	15.6

Table 7.

Age-hardening at 50° C.

No.	Brinell Hardness. (500 kg. Pressure, 10 mm. Ball, 30 sec.)				
	Immediately after.	2 hours after.	24 hours after.	Hardening in 24 hours.	
				Number.	Degree.
A 1	31.8	29.5	30.0	—	—
„ 2	32.2	31.8	36.6	4.4	15.7
„ 3	43.0	49.8	57.8	14.8	34.5
„ 4	61.0	70.0	80.3	19.3	31.6
„ 5	63 4	75.0	94.5	31.1	49.1
B 1	36.0	34.5	34.5	—	—
„ 2	39.8	43.5	45.0	5.2	13.1
„ 3	49.8	61.8	70.0	20 2	40.5
„ 4	57.0	67.0	78.2	21.2	37.2
„ 5	80.0	81.0	93.5	13.5	16.9
C 1	45.3	45.5	49.7	4.4	9.7
„ 2	57.0	54.3	56.2	—	—
„ 3	74.5	87.2	96.2	21.7	28.8
„ 4	77.5	78.5	85.5	8.0	10.3
„ 5	89.0	92.0	113 0	24.0	26.9
D 1	58.0	62.5	63.3	5.3	9.1
„ 2	65.5	67.5	78.5	13.0	19.7
„ 3	66.3	86.0	89.0	22 7	34.3
„ 4	90.2	104.0	107.5	17.3	19.2
„ 5	100.0	105.0	119.0	19.0	19.0

In these figures we see how ageing gave rise hardening to these series of alloys, when they were heated at 500° C. and quenched in water at 0°, 50°, 75°, and 100° C. respectively. Also it is seen how the degrees of hardening varied with the content of zinc in these series of alloys containing the same content of copper.

In the case of alloys containing 0.7 per cent. and 1.7 per cent. of

copper, age-hardening was observed in ageing at the lower temperature even in an alloy of less content of zinc, which did not show any indication of hardening in ageing at the higher temperature. At the same temperature hardening was found to take place with rapid increase of rate as the content of zinc increased, and a maximum degree of hardening was observed in a certain alloy. But the alloy which showed the maximum degree of hardening varied with the temperature of ageing.

Table 8.

Age-hardening at 75° C.

No.	Brinell Hardness. (500 kg. Pressure, 10 mm. Ball, 30 sec.)				
	Immediately after.	2 hours after.	24 hours after.	Hardening in 24 hours.	
				Number.	Degree.
A 1	28.6	27.6	28.3	—	—
„ 2	30.0	32.7	30.0	—	—
„ 3	38.5	44.2	53.5	15.0	38.9
„ 4	49.7	65.5	75.3	25.6	51.5
„ 5	57.7	77.0	86.0	23.3	49.0
B 1	31.3	33.0	31.8	—	—
„ 2	38.0	37.5	38.0	—	—
„ 3	50.0	48.0	54.8	4.8	9.6
„ 4	61.0	65.0	81.8	20.8	34.1
„ 5	74.5	83.7	91.5	17.0	22.9
C 1	38.0	39.0	38.3	—	—
„ 2	54.7	50.0	49.5	—	—
„ 3	61.0	74.0	80.0	19.0	31.2
„ 4	66.7	70.0	83.0	16.3	24.4
„ 5	80.8	85.0	89.2	8.4	10.4
D 1	44.3	48.5	51.0	6.7	15.1
„ 2	59.7	73.5	80.0	20.3	25.4
„ 3	68.0	72.2	77.8	9.8	11.5
„ 4	85.0	86.0	98.5	13.5	15.9
„ 5	91.0	96.0	113.0	22.0	24.2

Table 9.

Age-hardening at 100° C.

No.	Brinell Hardness (500 kg. Pressure, 10 mm. Ball, 30 sec.)				
	Immediately after.	2 hours after.	24 hours after.	Hardening in 24 hours.	
				Number.	Degree.
A 1	29.5	29.5	30.2	—	—
„ 2	30.3	31.2	30.0	—	—
„ 3	46.0	45.0	45.0	—	—
„ 4	59.0	70.5	86.0	27.0	45.7
„ 5	44.0	70.0	86.0	42.0	93.2
B 1	36.0	32.8	34.5	—	—
„ 2	35.0	34.8	35.5	—	—
„ 3	45.0	41.7	46.5	—	—
„ 4	36.0	60.0	89.0	53.0	147.2
„ 5	40.0	78.5	92.0	52.0	130.0
C 1	35.5	—	38.3	2.8	7.8
„ 2	50.0	50.0	48.0	—	—
„ 3	73.0	72.0	72.0	—	—
„ 4	51.0	49.5	50.0	—	—
„ 5	80.0	80.0	92.0	12.0	15.0
D 1	43.0	45.7	49.0	6.0	13.9
„ 2	53.0	50.0	56.8	3.8	7.2
„ 3	83.0	83.0	84.5	—	—
„ 4	105.0	105.0	116.5	11.5	10.9
„ 5	100.0	109.0	143.0	43.0	43.0

Compared with the case above mentioned, the degree of hardening was generally small in the case of the series containing about 3.15 per cent. and 4.6 per cent. of copper, and the relation of hardening in these series seems at the first sight to be much complicated, as shown in Figures.

It is seen, however, that the similar relation as above elucidated exists in each class of alloys, when these series are classified in 3 parts as divided by dotted lines in the figures.

Concerning the individual alloys we see also that a similar relation existed between the degree of hardening and the temperature of ageing, e. i., hardening took place over a certain range of temperature, and in this range there was a temperature, at which a maximum degree of hardening occurred, even if this phenomenon was not always marked in some alloys, for our experiments were excecuted only at the temperatures from 0° to 100° C.

CHANGE OF THERMAL EXPANSION PRODUCED IN QUENCHED SPECIMENS.

Age-hardening has been known to occur accompanying with some change of specific volume and electric resistivity[1]. Even if this change is very small in the case of ageing, the reaction would be accelerated by heating the quenched specimens again. The present purpose of experiment was to examine the phenomena of tempering by measuring the thermal expansion of quenched alloys on heating.

In the experiment we used the same specimens in a cylindrical form of 15 cm. in length and 6.5 mm. in diameter, which had been employed for the determination of solid transformation, as described in Part I. These specimens were quenched at 450° C. in water, and their thermal expansion was measured with a Honda's dilatometer. The heating rate was about 1° C. per minute.

Fig. 8 shows the results of the experiment. From the figure we see that in the alloy *ZC* 7 (*Cu* 3.37%, *Zn* 29.80%) the rate of expansion began to decrease slightly at about 80° C. and at about 150° C. the expansion commenced to slacken considerably. Subsequently it was changed into a rapid rate at about 180° C., and then it followed the normal course. The alloy *ZC* 6 (*Cu* 3.46%, *Zn* 24.26%) showed also a similar change of expansion.

But the other alloys containing less than 18 per cent. of zinc did not show such irregular change of expansion as in the former alloys, even

(1) S. Konno, Investigation of Metals, 2 (1924), 13.

Fig. 8.

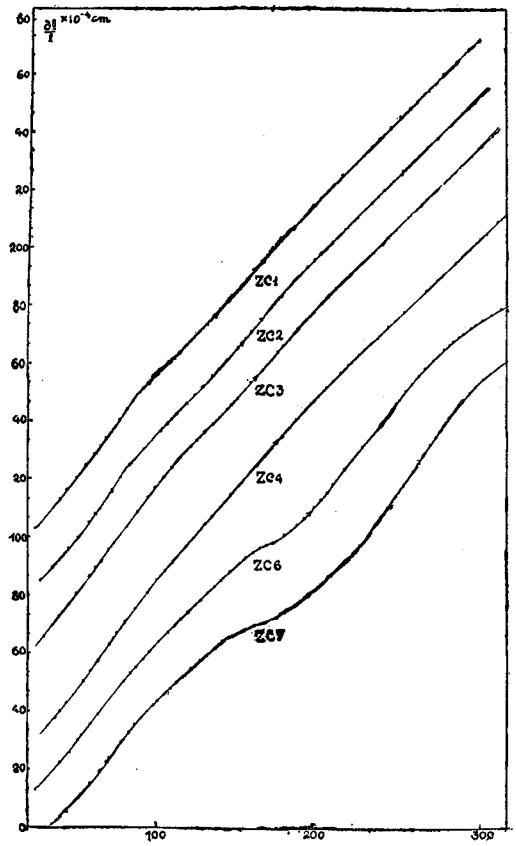

Temperature.

if some change of expansion was observed to take place from 50° to 200° C.

The alloy containing more than 18 per cent. of zinc shows a ternary peritectoid transformation at 292° C. in the state of equilibrium, but the reaction is in the most part suppressed by quenching at the higher temperature than that of the reaction.

When such a quenched alloy is heated again, it tries to attain to the state of lower temperature, and the reaction proceeds rapidly at a certain temperature. This is shown as the irregular change of expansion at about 180° C.

However, the alloys containing less than 18 per cent. of zinc did

not show any marked change of expansion. This is in the fact that the reactions to occur in these alloys are all concerned in the change of solubility of (γ), $CuAl$, or $CuAl_2$ in (α) and the transformation of $CuAl_2$ to $CuAl$.

Accordingly, we see that the degree of irregular change of expansion is not the direct indication of hardening, because age-hardening was not always distinguished in the alloys, which showed markedly the irregular change of expansion.

THEORETICAL CONSIDERATION OF AGE-HARDENING.

Concerning the age-hardening in *Al*-rich *Al-Zn* alloys the writer has already published an opinion[1] that age-hardening was such a phenomenon of the spontaneous crystallization of the second phase or phases in a super-cooled solid solution, as Tammann explained in a super-cooled liquid[2].

According to Tammann, the power of spontaneous crystallization in super-cooled liquid depends upon the temperature of super-cooling, and at a certain temperature of super-cooling the liquid solidifies with a maximum rate of crystallization. Here the power of crystallization means the numbers of centers of crystallization to be produced in unit volume per unit time. Also the linear velocity of crystallization reaches a maximum at a certain temperature of super-cooling. But their maximums do not always coincide with each other. (Fig. 9)

Fig. 9.

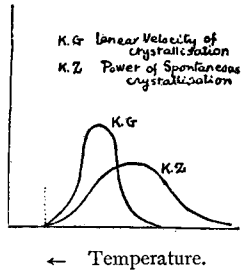

It is well known that an alloy, which shows age-hardening, consists at higher temperatures of a solid solution, and at lower temperatures the solid solution reaches the limit of solubility with regard to the second phase or phases. On slow cooling, therefore, the second phase or phases are separated gradually from the mother solid solution. When such an

(1) Op. Cit.
(2) Tammann, Metallograpy, 14.

alloy is quenched at a higher temperature, the solid solution, which is stable at that temperature, is changed into the state of super-saturation to the second phase or phases. Here arises a problem, if the separation of the second phase or phases is completely suppressed by quenching or not. Now we assume that the spontaneous separation of super-saturated phase or phases takes place in a certain range of temperatures as in super-cooled liquid, and age-hardening is a phenomenon which results from that spontaneous crystallization.

Granted that age-hardening is due to the spontaneous crystallization of solute phase or phases in super-cooled solid solution, the mechanism of hardening is another problem to be solved.

No matter how solute atoms may be arranged in the solvent lattices composing the solid solution, disintegration and rearrangement of the original lattices have to take place entirely or in some parts of the mother crystals, in order that the second phase or phases are separated from them. In this case the disintegration of lattices results in the refining of crystals, and the rapid change of lattice construction must produce some internal strain in the crystals. As well known, refining of crystals is one factor of hardening, and the existence of internal strain can be supposed to be another factor of hardening, as metals and metallic alloys can be strain-hardened by mechanical work.

On the other hand we must take the effects of softening into consideration. The higher the temperature of ageing, the more would the linear velocity of crystallization be accelarated, and the coagulation of the disintegrated mother crystals must occur at the same time. These effects result evidently in softening of alloys.

Furthermore, the degree of super-saturation can be said to be one factor of determining the degree of hardening, because the centers of crystallization may be the more produced in the solid solution, the more super-saturated it be.

Concerning a series of alloys, therefore, we see that age-hardening at a certain temperature occurs with a maximum rate in alloy of a certain composition and at another temperature the maximum hardening

is found to take place in alloy of another composition, as this relationship is illustrated in Fig. 10.

Fig. 10.

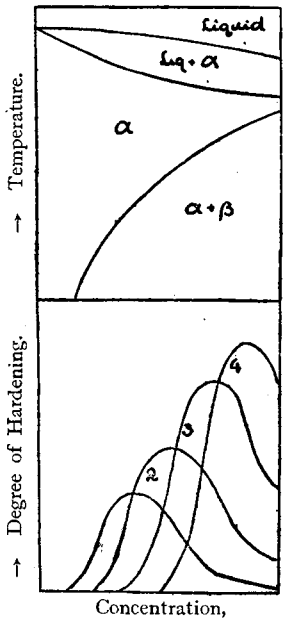

In our experiment such relationship was clearly observed to hold between concentration and the degree of hardening. For example, it will be seen in Figs. 4–5 that the series of alloys containing 0.7 and 1.7 per cent. of copper affords a fairly remarkable resemblance between the experiment and the theoretical explanation. Although the alloys above referred are of ternary composition, they may be assumed in these cases to be composed of binary elements, as the content of copper is very slight.

In the series of alloys containing about 3.15 per cent. and 4.6 per cent. of copper, however, this problem was not so simple as to consider them as a binary system. It has already been mentioned that these series must be classified in 3 parts, as shown in Figs. 6–7, and a similar relation as in a binary alloys holds in each part.

According to the equilibrium sections given in Part I, the alloys whose content of copper is 3 to 5 per cent. and whose content of zinc varies from zero to 20 per cent. may be classified in 4 kinds of alloys as follows;

(1) Alloys containing from zero to about 5 per cent. of zinc, which consist of $(\alpha)+CuAl_2$ only, even if the solubility of $CuAl_2$ in (α) varies with falling temperature.

(2) Alloys containing from about 5 to 10 per cent. of zinc, which consist of $(\alpha)+CuAl_2$ at higher temperature, but, on being slowly cooled, $CuAl_2$ is changed into $CuAl$. With further fall of temperature, (γ) and $CuAl$ are to be separated out of (α), although such a phase field is not shown in the equilibrium section. (In these sections the lowest temperature is 200° C.)

(3) Alloys containing from about 10 to 18 per cent. of zinc, which

consist of $(\alpha)+(\gamma)+CuAl$ at room temperature, $CuAl_2$ being converted into $CuAl$, and (γ) and $CuAl$ being separated from (α) with falling temperature.

(4) Alloys containing more than about 18 per cent. of zinc, in which $CuAl_2$ change into $CuAl$, (β) is separated from (α), and finally a non-variant reaction

$$(\beta)+CuAl \rightarrow (\alpha)+(\gamma)$$

takes place. At room temperature they consist of $(\alpha)+(\gamma)+CuAl$.

Accordingly, the phenomena of age-hardening in these series of alloys may be said to be different in each of these different kinds of alloys. In (1) the solubility of $CuAl_2$ in (α) is the only factor of hardening, but in (2) and (3) the chief cause of hardening is presumably in the fact that the solubility of (γ) and $CuAl$ in (α) väries markly with temperature, even if the transformation of $CuAl_2$ to $CuAl$ must be taken into consideration. In (4) the non-variant reaction

$$(\beta)+CuAl \rightleftarrows (\alpha)+(\gamma)$$

may be regarded to be a chief factor of hardening.

Among these reactions, however, the separation of (γ) and $CuAl$ from (α) is the most effective to give rise to hardening, as shown in Figs. 6—7.

In this way the complicated phenomena of age-hardening in these series will be easily understood on the standpoint of the constitution of alloys.

SUMMARY

In conclusion, the present experiments are summarized as follows:

(1) $L5$ alloy was quenched at various temperatures, and the phenomena of ageing were observed. The influence of quenching was marked in the alloy quenched at higher temperature, and hardening was found to be marked in the alloy containing less amount of copper. Also hardening was found to take place in two steps.

(2) The effect of tempering at 150°–200° C. was observed to result in softening of the alloys, but hardness and tensile strength were some-

what improved by tempering at 200°–300° C. The effect of tempering was marked in the alloy containing 3 per cent. of copper than that of less content of copper.

(3) Quenching was carried out of 4 series of alloys whose content of copper varied from 0 7 to 4.6 per cent , and whose content of zinc varied from 4 to 20 per cent. A complicated relation was found to exist between age-hardening and composition of alloys.

(4) Thermal expansion of quenched specimens were measured, and the irregular change of expansion was found not to be the direct indication of hardening due to tempering or ageing.

(5) Age-hardening was considered to be due to the spontaneous crystallization of solute phase or phases in a super-cooled solid solution. As the mechanism of hardening it was also considered that the separation of the second phase or phases accompanying with the disintegration of solvent lattices gave rise to hardening on one side, and on the other, internal strain produced in crystals, owing to the rapid change of lattice construction.

ACKNOWLEDGMENT.

In conclusion, the writer would like to express his cordial thanks to Professor D. Saito, under whose guidance the present experiments were carried out, and to Mr. T. Suzuki, who gave much assistance in this research and kindly analysed the alloys used in the present experiments.

The writer's thanks are also due to the Kaibo-Gikwai, a subsidy from which enabled his research to be undertaken.

Fig. 32.

General Equilibrium Diagram.

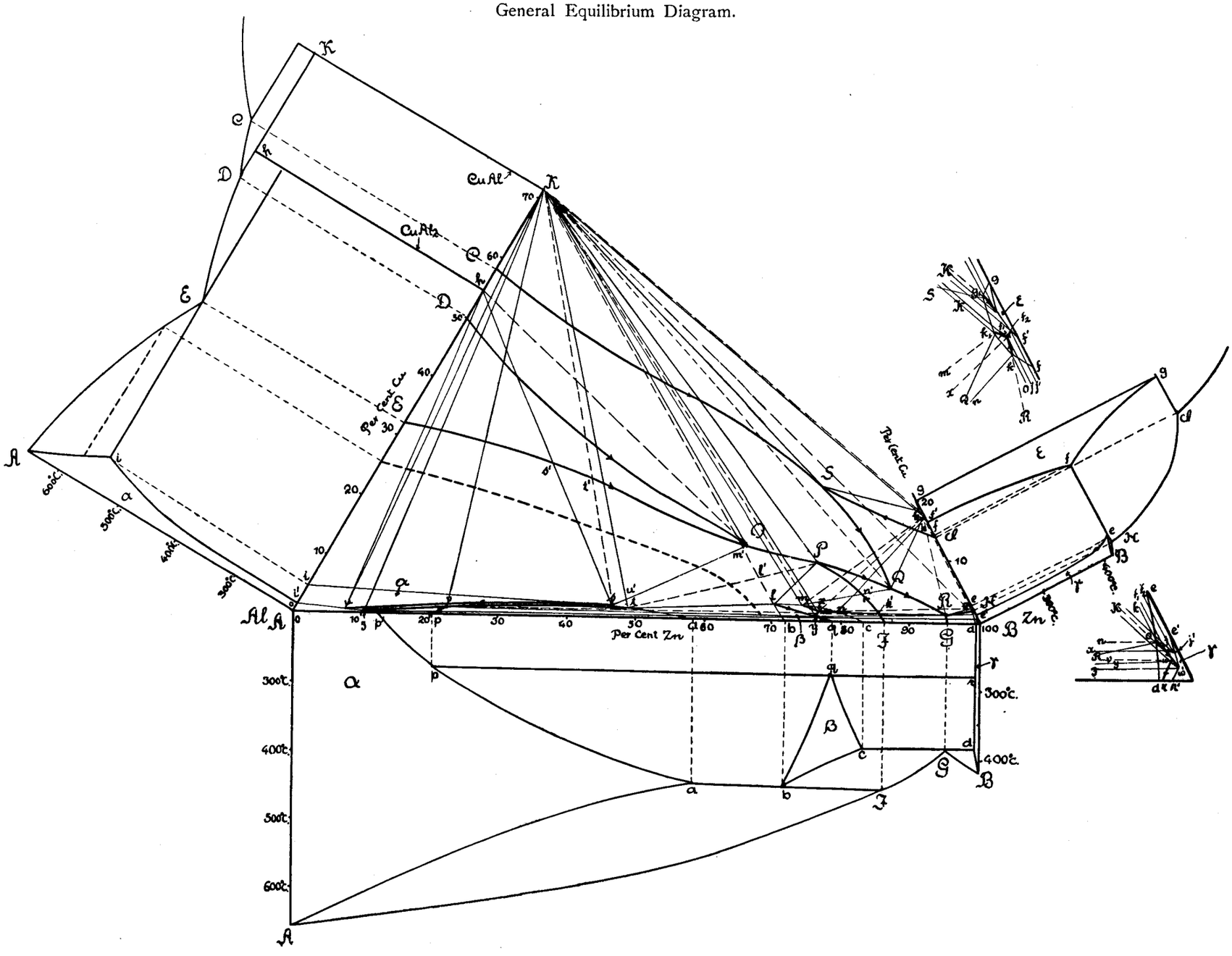

1. CZA 3 (Cu 0.69%, Zn 85.46%) chill cast. ×150

2. CZA 4 (Cu 0.84%, Zn 79.88%) chill cast. ×170

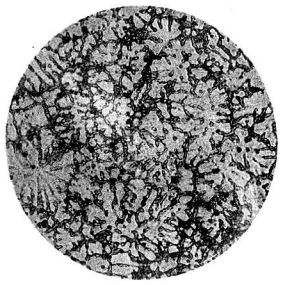

3. CZA 12 (Cu 3.76%, Zn 10.93%) chill cast. ×150

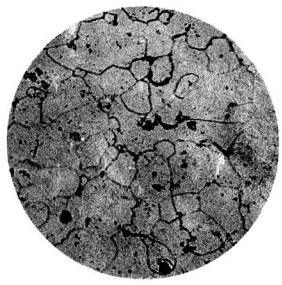

4. CZA 6 (Cu 1.29%, Zn 71.40%) quenched at 400°C. ×150

5. CZA 8 (Cu 2.08%, Zn 52.97%) quenched at 350°C. ×150

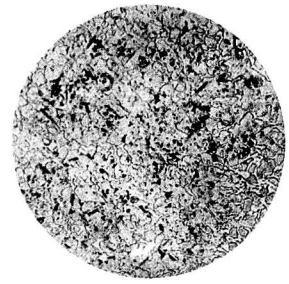

6. CZA 12 (Cu 3.76%, Zn 10.93%) quenched at 350°C. ×150

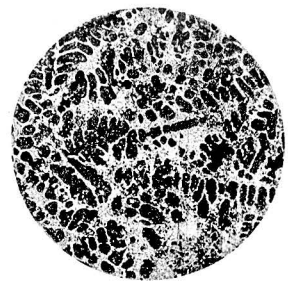

7. CZC 4 (Cu 2.62%, Zn 85.88%) chill cast. ×170

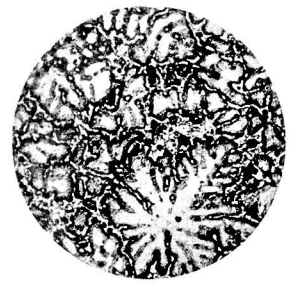

8. CZC 8 (Cu 7.87%, Zn 61.00%) chill cast. ×320

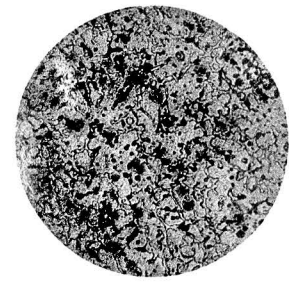

9. CZC 13 (Cu 15.59%, Zn 22.50%) quenched at 400°C. ×150

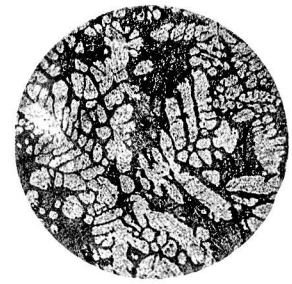

10. CZD 1 (Cu 1.49%, Zn 95.54%) chill cast. ×150

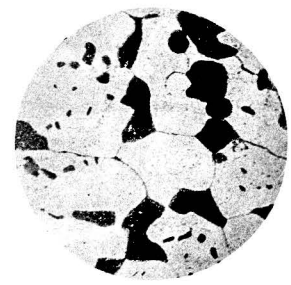

11. CZD 1 (Cu 1.49%, Zn 95.54%) quenched at 350°C. ×150

12. CZD 3 (Cu 4.51%, Zn 84.52%) chill cast. ×150

(Reduced to $\frac{2}{3}$ original size.)

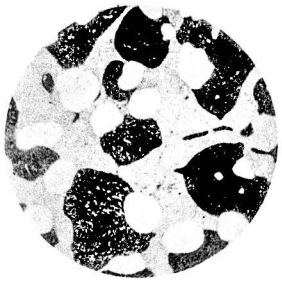

13. CZD 3 (Cu 4.51%, Zn 84.52%) quenched at 350°C. ×300

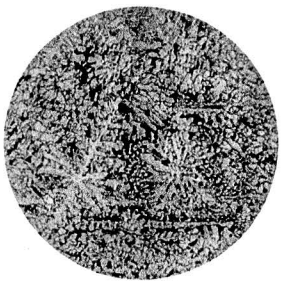

17. CZD 12 (Cu 23.57%, Zn 20.08%) chill cast. ×150

21. CZF 7 (Cu 17.88%, Zn 62.75%) chill cast. ×250

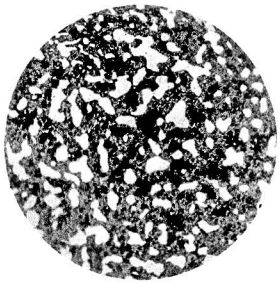

14. CZD 5 (Cu 7.38%, Zn 74.75%) quenched at 350°C. ×300

18. CZD 12 (Cu 23.57%, Zn 20.08%) quenched at 400°C. ×300

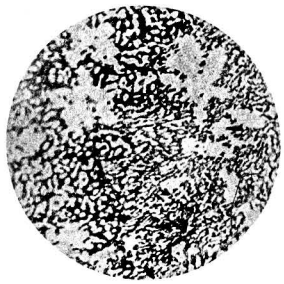

22. CZF 6 (Cu 16.01%, Zn 65.75%) quenched at 350°C. ×300

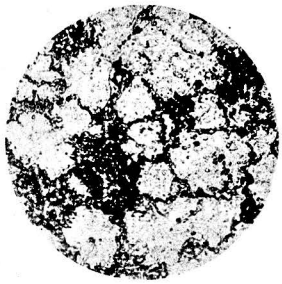

15. CZD 8 (Cu 11.95%, Zn 60.51%) quenched at 350°C. ×300

19. CZF 4 (Cu 8.94%, Zn 80.25%) chill cast. ×150

23. CZF 8 (Cu 19.37%, Zn 52.55%) quenched at 350°C. ×300

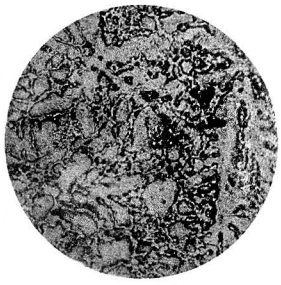

16. CZD 9 (Cu 14.70%, Zn 51.48%) chill cast. ×300

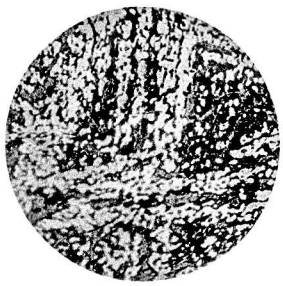

20. CZF 3 (Cu 6.82%, Zn 85.38%) quenched at 350°C. ×300

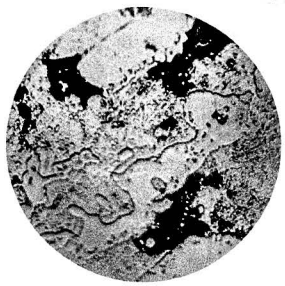

24. CZF 9 (Cu 27.10%, Zn 42.38%) quenched at 350°C. ×700

(Reduced to $\frac{2}{3}$ original size.)

25. CZF 12 (Cu 39.42%, Zn 12.13%) quenched at 350°C. ×300

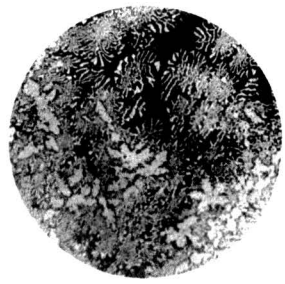

29. CZG 6 (Cu 14.90%, Zn 71.63%) chill cast. ×250

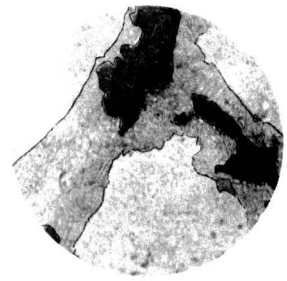

33. ZF 7 (Cu 9.60%, Zn 28.52%) quenched at 305°C. ×750

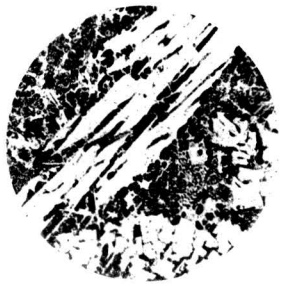

26. CZF 11 (Cu 35.32%, Zn 22.31%) chill cast. ×150

30. CZG 4 (Cu 10.30%, Zn 78.85%) quenched at 335°C. ×250

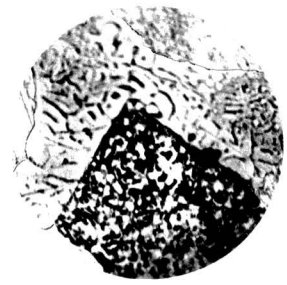

34. ZF 7 (Cu 9.60%, Zn 28.52%) quenched at 305°C. ×750

27. CZG 2 (Cu 4.75%, Zn 89.88%) chill cast. ×150

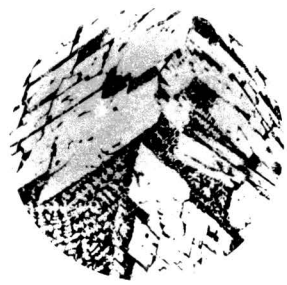

31. CZG 12 (Cu 39.45%, Zn 21.13%) chill cast. ×150

35. ZF 3 (Cu 10.09%, Zn 14.46%) quenched at 350°C. ×750

28. CZG 3 (Cu 7.33%, Zn 84.75%) chill cast. ×250

32. CZG 13 (Cu 44.25%, Zn 11.25%) chill cast. ×250

36. ZF 2 (Cu 9.90%, Zn 8.48%) quenched at 350°C. ×750

(Reduced to $\frac{2}{3}$ original size.)